

Integrated analysis of environmental and genetic influences on cord blood DNA methylation in new-borns

Running title: Combination of genetic and environmental effects best explain DNA cordblood methylation in variably methylated regions

Darina Czamara¹, Gökçen Eraslan^{2,3}, Christian M. Page^{4,5}, Jari Lahti^{6,7}, Marius Lahti-Pulkkinen^{6,8}, Esa Hämäläinen⁹, Eero Kajantie^{10,11,12}, Hannele Laivuori^{13,14,15,16}, Pia M Villa¹³, Rebecca M. Reynolds⁸, Wenche Nystad¹⁷, Siri E Håberg⁵, Stephanie J London¹⁸, Kieran J O'Donnell^{19,20}, Erika Garg¹⁹, Michael J Meaney^{19,20,21}, Sonja Entringer^{22,23}, Pathik D Wadhwa^{23,24}, Claudia Buss^{22,23}, Meaghan J Jones²⁵, David TS Lin²⁵, Julie L MacIsaac²⁵, Michael S Kobor²⁵, Nastassja Koen^{26,27}, Heather J Zar²⁸, Karestan C Koenen²⁹, Shareefa Dalvie²⁶, Dan J Stein^{26,27}, Ivan Kondofersky^{2,30}, Nikola S Müller², Fabian J Theis^{2,30}, Major Depressive Disorder Working Group of the Psychiatric Genomics Consortium[†], Katri Räikkönen⁶ and Elisabeth B Binder^{*1,31}.

¹ Max-Planck-Institute of Psychiatry, Department of Translational Research in Psychiatry, Munich, Germany

² Institute of Computational Biology, Helmholtz-Zentrum München, German Research Center for Environmental Health, Neuherberg, Germany

³ School of Life Sciences, Weihenstephan, Technische Universität München, Freising, Germany

⁴ Oslo Centre for Biostatistics and Epidemiology, Research Support Unit, Oslo University Hospital, Oslo, Norway

⁵ Center for Fertility and Health, Norwegian Institute of Public Health, Oslo, Norway

⁶ Department of Psychology and Logopedics, Faculty of Medicine, University of Helsinki, Finland

⁷ Helsinki Collegium for Advanced Studies, University of Helsinki, Finland

⁸ British Heart Foundation Centre for Cardiovascular Science, Queen's Medical Research Institute, University of Edinburgh, UK

⁹ HUSLAB and Department of Clinical Chemistry, Helsinki University, Helsinki, Finland

¹⁰ Oulu University Hospital and University of Oulu, PEDEGO Research Unit, MRC Oulu, Finland

- ¹¹ Hospital for Children and Adolescents, University of Helsinki and Helsinki University Hospital, Finland
- ¹² National Institute for Health and Welfare, Helsinki, Finland
- ¹³ Medical and Clinical Genetics and Obstetrics and Gynaecology University of Helsinki and Helsinki University Central Hospital, Finland
- ¹⁴ Institute for Molecular Medicine Finland, Helsinki Institute of Life Science, University of Helsinki, Finland
- ¹⁵ Faculty of Medicine and Life Sciences, University of Tampere, Tampere, Finland
- ¹⁶ Department of Obstetrics and Gynecology, Tampere University Hospital, Tampere, Finland
- ¹⁷ Department of Chronic Diseases and Ageing, Norwegian Institute of Public Health, Oslo, Norway
- ¹⁸ Epidemiology Branch, National Institute of Environmental Health Sciences, National Institutes of Health, U.S. Department of Health and Human Services, Research Triangle Park, North Carolina, United States of America
- ¹⁹ Ludmer Centre for Neuroinformatics and Mental Health, Douglas Mental Health University Institute, McGill University, Montreal, QC, Canada
- ²⁰ Sackler Program for Epigenetics and Psychobiology at McGill University, Montreal, QC, Canada
- ²¹ Singapore Institute for Clinical Sciences, Singapore
- ²² Charité – Universitätsmedizin Berlin, corporate member of Freie Universität Berlin, Humboldt-Universität zu Berlin, and Berlin Institute of Health (BIH), Institute of Medical Psychology, Berlin, Germany
- ²³ University of California, Irvine, Development, Health, and Disease Research Program, Orange, CA, USA
- ²⁴ Departments of Psychiatry and Human Behavior, Obstetrics and Gynecology, and Epidemiology, University of California, Irvine, School of Medicine, Irvine, CA, USA
- ²⁵ Centre for Molecular Medicine and Therapeutics, Department of Medical Genetics, University of British Columbia and the BC Children's Hospital Research Institute, Vancouver, BC, Canada
- ²⁶ Department of Psychiatry and Mental Health, University of Cape Town, South Africa
- ²⁷ South African Medical Research Council (SAMRC), Unit on Risk and Resilience in Mental Disorders, Cape Town, South Africa
- ²⁸ Department of Paediatrics & Child Health and SAMRC Unit on Child and Adolescent Health, University of Cape Town, South Africa
- ²⁹ Department of Epidemiology, Harvard T. H. Chan School of Public Health, Boston, MA, USA
- ³⁰ Department of Mathematics, Technische Universität München, Munich, Germany.
- ³¹ Department of Psychiatry and Behavioral Sciences, Emory University School of Medicine, USA

† A full list of consortium members appears at the end of the paper.

Correspondence and requests for materials should be addressed to Elisabeth B. Binder (email: binder@psych.mpg.de).

Key words: cord blood, DNA methylation, variably methylated regions (VMRs), prenatal environment, epigenetics, methylation quantitative trait loci (meQTL), gene x environment interaction

Abstract

Epigenetic processes, including DNA methylation (DNAm), are among the mechanisms allowing integration of genetic and environmental factors to shape cellular function. While many studies have investigated either environmental or genetic contributions to DNAm, few have assessed their integrated effects. Here we examine the relative contributions of prenatal environmental factors and genotype on DNA methylation in neonatal blood at variably methylated regions (VMRs) in 4 independent cohorts (overall n=2,365). We use Akaike's information criterion to test which factors best explain variability of methylation in the cohort-specific VMRs: several prenatal environmental factors (E), genotypes in cis (G), or their additive (G+E) or interaction (GxE) effects. Genetic and environmental factors in combination best explain DNAm at the majority of VMRs. The CpGs best explained by either G, G+E or GxE are functionally distinct. The enrichment of genetic variants from GxE models in GWAS for complex disorders supports their importance for disease risk.

93 **Introduction**

94 Fetal or prenatal programming describes the process by which environmental events during
95 pregnancy influence the development of the embryo with on-going implications for future health
96 and disease. Several studies have shown that the *in utero* environment is associated with disease
97 risk, including coronary heart disease ^{1,2}, type 2 diabetes ³, childhood obesity ^{4,5} as well as
98 psychiatric problems ⁶ and disorders ⁷⁻⁹.

99 Environmental effects on the epigenome, for example via DNA methylation, could lead to
100 sustained changes in gene transcription and thus provide a molecular mechanism for the
101 enduring influences of the early environment on later health ¹⁰. Smoking during pregnancy
102 influences widespread and highly reproducible differences in DNA methylation at birth ¹¹. Less
103 dramatic effects have been reported for maternal body mass index (BMI) ¹², pre-eclampsia and
104 gestational diabetes ^{13,14}. Possible epigenetic changes as a consequence of prenatal stress are less
105 well established ¹⁵. Some of these early differences in DNA methylation persist, although
106 attenuated, through childhood ^{11,16} and might be related to later symptoms and indicators of
107 disease risk, including BMI during childhood ^{17,18} or substance use in adolescence ¹⁹. These data
108 emphasize the potential importance of the prenatal environment for the establishment of inter-
109 individual variation in the methylome as a predictor or even mediator of disease risk trajectories.
110 In addition to the environment, the genome plays an important role in the regulation of DNA
111 methylation. To this end, the impact of genetic variation, especially of single nucleotide
112 polymorphisms (SNPs) on DNA methylation in different tissues, has resulted in the discovery of
113 a large number of methylation quantitative trait loci (meQTLs, i.e., SNPs significantly associated
114 with DNA methylation status ²⁰). These variants are primarily in cis, i.e., at most 1 million base
115 pairs away from the DNA methylation site ²⁰⁻²² and often co-occur with expression QTLs or

other regulatory QTLs²³⁻²⁵. The association of meQTLs with DNA methylation is relatively stable throughout the life course²¹. In addition, SNPs within meQTLs are strongly enriched for genetic variants associated with common disease in large genome-wide association studies (GWAS) such as BMI, inflammatory bowel disease, type 2 diabetes or major depressive disorder^{21,23,24,26}.

Environmental and genetic factors may act in an additive or multiplicative manner to shape the epigenome to modulate phenotype presentation and disease risk²⁷. However, very few studies have so far investigated the joint effects of environment and genotype on DNA methylation, especially in a genome-wide context. Klengel et al.²⁸, for instance, reported an interaction of the FK506 binding protein 5 gene (*FKBP5*) SNP genotype and childhood trauma on *FKBP5* methylation levels in peripheral blood cells, with trauma associated changes only observed in carriers of the rare allele. The most comprehensive study of integrated genetic and environmental contributions to DNA methylation so far was performed by Teh et al.²⁹. This study examined variably methylated regions (VMRs), defined as regions of consecutive CpG-sites showing the highest variability across all methylation sites assessed on the Illumina Infinium HumanMethylation450 BeadChip array. In a study of 237 neonate methylomes derived from umbilical cord tissue, the authors explored the proportions of the influence of genotype vs. prenatal environmental factors such as maternal BMI, maternal glucose tolerance and maternal smoking on DNA methylation at VMRs. They found that 75% of the VMRs were best explained by the interaction between genotype and environmental factors (GxE) whereas 25% were best explained by SNP genotype and none by environmental factors alone. Collectively, these studies highlight the importance of investigating the combination of environmental and genetic contributions to DNA methylation and not only their individual contribution.

139 The main objective of the present study is to extend our knowledge of combined effects of
140 prenatal environment and genetic factors on DNA methylation at VMRs. Specifically, this is
141 addressed by: 1) assessing the stability of the best explanatory factors across different cohorts
142 and whether this extends to all environmental factors, 2) dissecting differences between additive
143 and interactive effects of gene and environment not explored in Teh et al., 3) testing whether
144 VMRs influenced by genetic and/or environmental factors might have a different predicted
145 impact on gene regulation and 4) evaluating the relevance of genetic variants that interact with
146 the environment to shape the methylome for their contribution to genetic disease risk.

147 Our results show that across cohorts genetic variants in combination with prenatal environment
148 are the best predictors of variance in DNA methylation. We observe functional differences of
149 both the genetic variants and the methylation sites best explained by genetic or additive and
150 interactive effects of genes and environment. Finally, the enrichment of genetic variants within
151 additive as well as interactive models in GWAS for complex disorders supports the importance
152 of these environmentally modified methylation quantitative trait loci for disease risk.

Results

Cohorts and analysis plan

We investigated the influence of the prenatal environment and genotype on VMRs in the DNA of 2,365 newborns within 4 different cohorts: Prediction and Prevention of Pre-eclampsia and Intrauterine Growth Restrictions (PREDO, cordblood)³⁰, the UCI cohort (³¹⁻³³, heel prick), the Drakenstein Child Health Study (DCHS, cordblood)^{34,35} and the Norwegian Mother and Child Cohort Study (MoBa, cordblood³⁶). A description of the workflow of this manuscript is given in Figure 1 and the details for each of the cohorts are given in Table 1.

Table 1: overview of investigated cohorts

cohort	PREDO I	PREDO II	DCHS I	DCHS II	UCI	MoBa
sample-size	817	146	107	151	121	1,023
methylation array	Illumina 450K	Illumina EPIC	Illumina 450K	Illumina EPIC	Illumina EPIC	Illumina 450K
Methylation data processing	Funnorm and Combat	Funnorm and Combat	SWAN and Combat	BMIQ and Combat	Funnorm and Combat	BMIQ and Combat
SNP genotyping	Illumina Human Omni Express Exome	Illumina Human Omni Express Exome	Illumina PsychArray	Illumina GSA	Illumina Human Omni Express	Illumina HumanExome Core
infant gender male	433 (53.0%)	75 (51.4%)	63 (58.8%)	83 (55.0%)	65 (53.7%)	478 (46.7%)
maternal age mean (sd)	33.28 (5.79)	32.25 (4.92)	26.27 (5.87)	27.42 (5.93)	28.47 (4.91)	29.92 (4.32)
partity mean (sd)	1.05 (1.02)	0.87 (1.03)	0.98 (1.12)	1.09 (1.07)	1.11 (1.15)	0.83 (0.88)
Caesarian section	169 (20.7%)	36 (24.7%)	19 (17.6%)	35 (23.2%)	37 (30.6%)	228 (22.3%)
pre-pregnancy BMI mean (sd)	27.42 (6.40)	25.37 (5.79)	not available	not available	27.90 (6.44)	24.05 (4.19)
maternal smoking yes	exclusion criterion	exclusion criterion	7.40 (10.52) ^{a)}	4.94 (9.43) ^{a)}	10 (8.2%)	148 (14.4%)
gestational diabetes yes	183 (22.4%)	19 (13.0%)	no cases available	no cases available	9 (7.4%)	15 (1.5%)
hypertension yes	275	31 (21.2%)	2 (.19%)	2 (1.3%)	7 (5.8%)	50 (4.9%)

	(33.7%)					
betamethasone treatment yes	35 (4.3%)	2 (1.5%)	not available	not available	no cases available	not available
anxiety score mean (sd)	33.93 (7.90) ^{b)}	34.43 (8.38) ^{b)}	5.70 (4.15) ^{c)}	5.32 (3.91) ^{c)}	1.67 (0.41) ^{d)}	4.79 (1.36) ^{e)}
depression score mean (sd)	11.34 (6.47) ^{f)}	11.53 (6.98) ^{f)}	17.64 (12.10) ^{g)}	12.52 (11.55) ^{g)}	0.68 (0.41) ^{h)}	5.24 (1.57) ^{e)}

^{a)} based on ASSIST Tobacco Score

^{b)} STAI sum scores

^{c)} SRQ-20

^{d)} STAI average scores

^{e)} based on Hopkins Symptom Checklist

^{f)} CESD sum scores

^{g)} BDI-II

^{h)} CESD average score

We analyzed 963 cord blood samples from the PREDO cohort with available genome-wide DNA methylation and genotype data. Of these samples, 817 had data on the Illumina 450k array (PREDO I) and 146 on the Illumina EPIC array (PREDO II). The main analyses are reported for PREDO I, and replication and extension of the results is shown for PREDO II as well as for three independent cohorts including 121 heel prick samples (UCI cohort, EPIC array) as well as 258 (DCHS, 450K and EPIC array) and 1,023 cord blood samples (MoBa, 450K array). We tested ten different prenatal environmental factors covering a broad spectrum of prenatal phenotypes (see Table 1) (referred to as E), as well as cis SNP genotype (referred to as G), i.e., SNPs located in at most 1MB distance to the specific CpG, additive effects of cis SNP genotype and prenatal environment (G+E) and cis SNP x environment interactions (GxE) for association with DNA methylation levels (see Figure 1). We then assessed for each VMR independently which model described the variance of DNAm best using Akaike's information criterion (AIC) ³⁷. In all models, we corrected for child's gender, ethnicity (using MDS-components), gestational age as well as estimated cell proportions to account for cellular heterogeneity.

Variably Methylated Regions

We first identified candidate VMRs, defined as regions of CpG-sites showing the highest variability across all methylation sites. In PREDO I, we identified 10,452 variable CpGs that clustered into 3,982 VMRs (see Supplementary Data 1). Most VMRs (n=2,683) include 2 CpGs. As detailed in Supplementay Note 1, the distribution of methylation levels of CpGs within these VMRs is unimodal, (see Supplementary Figure 1A), VMRs are enriched in specific functional regions of the genome, correlate with differences in gene expression, and overlap with sites associated with specific prenatal environmental factors.

To examine the factors that best explain the variance in methylation in these functionally relevant sites, we chose the CpG-site with the highest MAD-score as representative of the VMR. These CpGs are named tagCpGs. The correlation between methylation levels of tagCpG and average methylation of the respective VMR was high (mean $r=0.85$, sd $r=0.08$), suggesting that the tag CpGs are valid representatives of their VMRs. Furthermore, tagCpGs are mainly uncorrelated with each other (mean $r=0.03$, sd=0.12).

Which models explain methylation of tagCpGs best?

We next compared the fit of four models for each of the 3,982 tagCpGs (see Figure 1): best SNP (G model), best environment (E model), SNP + environment (G+E model) and SNP x environment (GxE model). Association results for each model are listed in Supplementary Data 2-5. For each tagCpG, the model with the lowest AIC was chosen as the best model (see Methods section). In total, 40.6% of tagCpGs were best explained by GxE (n=1,616), followed by G (30%, n=1,194) and G+E (29%, n=1,171) (Figure 2A). E explained most variance in one tagCpG. All tag CpGs and the respective SNPs and environments from the best model are listed in Supplementary Data 6-8 and Supplementary Table 1.

With regard to environmental factors, 27.0% of tagCpGs best explained by the G+E model were associated with environmental factors related with stress or, in particular, glucocorticoids (i.e., maternal betamethasone treatment), 40.8% with general maternal factors (mostly maternal age) and 32.20 % with factors related to metabolism (pre-pregnancy BMI, hypertension, gestational diabetes). For best model GxE tagCpGs, the proportions of environmental factors were similar with 22.2%, 44.1% and 33.7%, respectively (see Figure 2B).

We next looked into the delta AIC, i.e., the difference between the AIC of the best model to the AIC of the next best model (see Supplementary Note 2). GxE models appear to be winning by a significantly larger AIC margin over the next best model, when compared to the other types of winning models (see Figure 2C).

DeepSEA prediction of SNP function

We were next interested in understanding the functionality of both the VMRs as well as the associated SNPs in the G, GxE and G+E models. For this we restricted the analyses only to potentially functional relevant SNPs using DeepSEA³⁸ and not all linkage disequilibrium (LD)-pruned SNPs as described above. DeepSEA, a deep neural network pretrained with DNase-seq and ChIP-seq data from the ENCODE³⁹ project, predicts the presence of histone marks, DNase hypersensitive regions (DHS) or TF binding for a given 1kb sequence. The likelihood that a specific genetic variant influences regulatory chromatin features is estimated by comparing predicted probabilities of two sequences where the bases at the central position are the reference and alternative alleles of a given variant. We reran the four models now restricting the cis-SNPs to those 36,241 predicted DeepSEA variants that were available in our imputed, quality-controlled genotype dataset.

Top results for models including G, GxE and G+E are depicted in Supplementary Data 9-12. Results were comparable to what we observed before: 1,195 (30.09%) of tagCpGs presented with best model G, 1,193 CpGs (30.04%) with best model G+E, 1,510 CpGs (38.02 %) with best model GxE and 74 CpGs (1.86%) with best model E (Figure 3A) and also showed similar differences in delta-AIC and proportions of E categories (see Supplementary Note 3). Only 10 tagCpGs did not present with any DeepSEA variant within 1MB distance in cis and were therefore not further considered. All respective CpG-environment-DeepSea SNP-combinations are depicted in Supplementary Data13-16.

The distribution of best models was not influenced by the degree of variability of DNA methylation, but was comparable across the whole range of DNA methylation variation (see Supplementary Note 4 and Supplementary Figure 2). A slight enrichment for G+E models was observed in longer VMRs with at least 3 CpGs ($p=9.00 \times 10^{-06}$, OR=1.39, Fisher-test, see Supplementary Figure 3).

In conclusion, also when we focus on potentially functionally relevant SNPs, it is the combination of genotype and environment which best explains VMRs.

We observed that, as expected, different types of exposures or maternal factors have different relative impact on DNA methylation (see Supplementary Note 5). However, even for those exposures with the highest fraction of VMRs best explained by E alone, combined models of G+E and GxE remain the best models in even higher fractions of VMRs (see Supplementary Figure 4B).

Functional annotation of different best models

256 Focusing on combinations between tagCpGs, environmental factors and DeepSEA variants, we
 257 found functional differences for both the SNPs as well as the tagCpGs (see Supplementary Note
 258 6) within the different models. Overall, 895 DeepSEA variants were uniquely involved in best G
 259 models, 905 were uniquely in best G+E models and 1,162 uniquely in best GxE models. As a
 260 DeepSEA variant can be in multiple 1 MB-cis windows around the tagCpGs, several DeepSEA
 261 variants were involved in multiple best models: 138 DeepSEA variants overlapped between G
 262 and GxE, 118 between G and G+E and 147 between GxE and G+E VMRs. We observed no
 263 significant differences with regard to gene-centric location for DeepSEA variants involved only
 264 in G models, only in G+E models or in multiple models. However, DeepSEA variants involved
 265 only in GxE models were significantly depleted for promoter locations ($p=3.92 \times 10^{-02}$,
 266 OR=0.79, Fisher-test, see Supplementary Figure 5A).
 267 Although no significant differences were present, DeepSEA SNPs involved in the G and G+E
 268 model were located in closer proximity to the specific CpG (model G: mean absolute
 269 distance=256.8 kb, sd=291.2 kb, model G+E: mean absolute distance =244.8 kb, sd=284.0 kb,
 270 Supplementary Figure 5B) whereas DeepSEA SNPs involved in GxE models (mean absolute
 271 distance =352.6 kb, sd=305.3 kb) showed broader peaks around the CpGs.
 272 With regards to histone marks, DeepSEA variants in general were enriched across multiple
 273 histone marks indicative of active transcriptional regulation (Figure 4C). DeepSEA variants
 274 involved in best model G+E showed further enrichment for strong transcription ($p=7.19 \times 10^{-03}$,
 275 OR=1.34, Fisher-test) as well as depletion for quiescent loci ($p=7.17 \times 10^{-03}$, OR=0.78, Fisher-
 276 test). In contrast, GxE DeepSEA variants were significantly enriched in these regions
 277 ($p=2.62 \times 10^{-02}$, OR=1.22, Fisher-test, Figure 4D).

Taken together, these analyses indicate that both the genetic variants and the VMRs in the different best models (G, GxE and G+E) preferentially annotate to functionally distinct genomics regions.

Replication of best models in independent cohorts

To assess whether the relative distribution of the best models for VMRs and DeepSEA variants was stable across different samples, we assessed the relative distribution of these models in 3 additional samples (DCHS I and DCHS II, UCI and PREDOII) with VMR data both from the Illumina 450K as well as the IlluminaHumanEPIC arrays. Information on these cohorts is summarized in Table 1 and the number of VMRs, the distribution of VMR methylation levels, VMR length and specific SNP information are given in Supplementary Note 7 and Supplementary Figure 6.

While major maternal factors overlapped among the cohorts - such as maternal age, delivery method, parity and depression during pregnancy - there were also differences, as the non-PREDO cohorts did not include betamethasone treatment but additionally included maternal smoking (see Table 1). Despite these differences and differences in the total number of VMRs, the overall pattern remained stable: in all 4 analyses, DCHS I, DCHS II, UCI and PREDO II, we replicated that E alone models almost never explained most of the variances, while G alone models explained the most variance in up to 15% of the VMRs; G+E in up to 32%; and GxE models in up to 60% (see Figure 5 and Table 2).

Table 2: VMRs and best models across cohorts

cohort	PREDO I	PREDO II	DCHS I	DCHS II	UCI
sample-size	817	146	107	151	121
methylation array	Illumina 450K	Illumina EPIC	Illumina 450K	Illumina EPIC	Illumina EPIC

# VMRs	3,972	8,547	6,072	10,005	9,525
proportion: best model E	2.0%	<1%	<1%	<1%	4.1%
best model G	30.0%	15.0%	15.8%	11.5%	12.8%
best model G+E	30.0%	29.0%	29.8%	32.1%	24.1%
best model GxE	38.0%	56.0%	54.3%	56.3%	59.0%

The importance of including G for a best model fit could also be observed for maternal smoking, described as one of the most highly replicated factors shaping the newborns' methylome¹¹ and present in the replication but not the discovery cohort PREDO I. These analyses are detailed in Supplementary Note 8.

We were also able to replicate our finding showing that GxE VMRs were enriched for OpenSea positions with a trend on the 450K array (DCHS I, OR=1.11, $p=5.03 \times 10^{-02}$, Fisher-test) and significantly for the EPIC array data (PREDOII: $p=2.96 \times 10^{-06}$, OR=1.29, UCI: $p=3.79 \times 10^{-02}$, OR=1.09, DCHSII: $p=2.91 \times 10^{-04}$, OR=1.16, Fisher-tests). For all additional cohorts, the delta AIC for best model GxE to the next best model was also significantly higher as compared to CpGs with G, E or G+E as the best model.

Overall, 387 tag CpGs overlapped between PREDO I, PREDO II, DCHS I and DCHS II (see Supplementary Figure 7), which allowed us to test the consistency of the best models for specific VMRs across the different cohorts. Over 70% of the overlapping tagCPGs showed consistent best models in at least 3 cohorts (see Figure 6) with GxE being the most consistent model (for over 60% of consistent models, see Supplementary Figure 8). Focusing only on EPIC data (PREDO II, DCHSII and UCI), we identified more, namely 2,091, tag CpGs that overlap across the three cohorts and here 86% show a consistent best model in at least two of the three cohorts, despite differences in study design, prenatal phenotypes and ethnicity.

Thus, the additional cohorts not only showed a consistent replication of the proportion of the models best explaining variance of VMRs but also consistency of the best model for specific

VMRs. Within this context, we observed the GxE models were the most consistent models across the cohorts (, see Supplementary Figure 8), with 85% of the CpGs with consistent models across 5 cohorts having GxE as the best model. Furthermore, we could validate specific GxE combinations between PREDO I and MoBa as shown as in the Supplementary Note 9.

Disease relevance

Finally, we tested whether functional DeepSEA SNPs involved in only G, only GxE and only G+E models in PREDO I for their enrichment in GWAS hits. We used all functional SNPs and their LD proxies (defined as r^2 of at least 0.8 in the PREDO cohort and in maximal distance of 1MB to the target SNP) and performed enrichment analysis with the overlap of nominal significant GWAS hits. We selected for a broad spectrum of GWAS, including GWAS for complex disorders for which differences in prenatal environment are established as risk factors, but also including GWAS on other complex diseases. For psychiatric disorders, we used summary statistics of the Psychiatric Genomics Consortium (PGC) including association studies for autism⁴⁰, attention-deficit-hyperactivity disorder⁴¹, bipolar disorder⁴², major depressive disorder⁴³, schizophrenia⁴⁴ and the cross-disorder associations including all five of these disorders⁴⁵. Additionally, we included GWAS of inflammatory bowel disease⁴⁶, type 2 diabetes⁴⁷ and for BMI⁴⁸. Nominal significant GWAS findings were enriched for DeepSEA variants and their LD proxies per se across psychiatric as well as non-psychiatric diseases (Figure 7A). However, G, GxE and G+E DeepSEA variants showed a differential enrichment pattern above all DeepSEA variants (Figure 7B), with strongest enrichments of GxE DeepSEA variants in GWAS of autism spectrum disorder ($p < 2.20 \times 10^{-16}$, OR=2.07 above DeepSEA, Fisher-test), attention-deficit-hyperactivity disorder ($p < 2.20 \times 10^{-16}$, OR=1.71, Fisher-test) and inflammatory

bowel disease ($p < 2.20 \times 10^{-16}$, OR=1.71, Fisher-test) and G+E DeepSEA variants in GWAS for attention-deficit-hyperactivity disorder ($p = 9.54 \times 10^{-36}$, OR=1.23, Fisher-test) and inflammatory bowel disease ($p = 1.85 \times 10^{-52}$, OR=1.30, Fisher-test). While SNPs with strong main meQTL effects such as those within G and G+E models have been reported to be enriched in GWAS for common disease, we now also show this for SNPs within GxE models that often have non-significant main G effects.

Discussion

We evaluated the effects of prenatal environmental factors and genotype on DNA methylation at VMRs identified in neonatal blood samples. We found that most variable methylation sites were best explained by either genotype and prenatal environment interactions (GxE) or additive effects (G+E) of these factors, followed by main genotype effects. This pattern was replicated in independent cohorts and underscores the need to consider genotype in the study of environmental effects on DNA methylation.

In fact, VMRs best explained by G, G+E or GxE and their associated functional genetic variants were located in distinct genomic regions, suggesting that different combinatorial effects of G and E may impact VMRs with distinct downstream regulatory effects and thus possibly context-dependent impact on cellular function. We also observed that functional variants with best models G, G+E or GxE, all showed significant enrichment within GWAS signals for complex disorders beyond the enrichment of the functional variants themselves. While this was expected for G and G+E models based on results from previous studies^{21,23,24,26}, it was surprising for GxE SNPs, as these often do not have highly significant main genetic effects. Their specific enrichment in GWAS for common disorders supports the importance of these genetic variants

that moderate environmental impact both at the level of DNA methylation but also, potentially, for disease risk.

The fact that GxE and G+E best explained the majority of VMRs (see Figure 5) and that GxE models were selected by a larger margin than the other models (see Figure 2C) was consistently found across all tested cohorts. These findings are in line with a previous report by Teh et al.²⁹ who performed a similar analysis based on AIC in umbilical cord tissue. Differences to the findings by Teh et al. are discussed in the Supplemental Discussion. Using data from 4 different cohorts, we not only saw comparable proportions of VMRs best explained by the different models, but also saw in the VMRs common across cohorts that specific VMRs had consistent best models (see Figure 6). This is in line with the fact that VMRs best explained by G, GxE or G+E show functional differences and may differentially impact gene regulation.

In addition to consistent findings using AIC-based approaches, we also observed some indication for validation of individual GxE and G+E combinations on selected VMRs using p-value based criteria, with a small number of specific G+E and GxE effects on VMRs replicating between the PREDO I and the MoBa cohort. The low number of specific replications could be due to lack of overall power as well as larger differences in prenatal factors between these two cohorts (see Table 1). As shown in Supplementary Figure 4B, which specific G and E combinations best explain VMRs is also dependent on the specific prenatal factors. Larger and more homogenous cohorts regarding exposures will be needed for such analyses to be more conclusive.

While E alone was rarely the best model, it should be pointed out that main environmental effects on DNA methylation were observed (see Supplementary Data 3), and consistent with previous large meta-analyses such as in the case of maternal smoking (see Supplementary Notes 7). Within the MoBa cohort, the cohort with the largest proportion of maternal smoking, 10% of

all tagCpGs were best explained by maternal smoking alone. However, in all other cohorts, where smoking was less prevalent, the inclusion of genotypic effects in addition to maternal smoking explained more of the variance. This supports that while main E effects on the newborn methylome are present, genotype is an important factor that, in combination with E, may explain even more of the variance in DNA methylation.

VMRs best explained by either E, G, G+E or GxE and their associated functional SNPs were enriched for distinct genomics locations and chromatin states (see Figure 4), suggesting that VMRs moderated by different combinations of G and E may in fact have distinct functional roles in gene regulation. Overall, VMRs best explained by GxE were consistently enriched for regions annotated to the OpenSea regions with lower CpG density and located farthest from CpG Islands⁴⁹. Open Sea regions have been reported to be enriched for environmentally-associated CpGs with for example exposure to childhood trauma⁵⁰ and may harbor more long-range enhancers.

In addition to their position relative to CpG islands and their CpG content, G, GxE and G+E VMRs and their associated functional SNPs also showed distinct enrichments for chromatin marks. Compared to 450K VMRs in general, VMRs with GxE as the best models were relatively depleted in regions surrounding the TSS, while VMRs with G+E were relatively enriched in these regions (see Figure 4), suggesting that GxE VMRs are located at more distance from the TSS than G+E VMRs. To better map the potential functional variants in these models and to compare methylation-associated SNPs from a regulatory perspective, we used DeepSEA³⁸, a machine learning algorithm that predicts SNP functionality from the sequence context based on sequencing data for different regulatory elements in different cell lines using ENCODE data³⁹.

We identified the SNPs with putatively functional consequences on regulatory marks by DeepSEA and compared putative regulatory effects of G, G+E and GxE hits. Relative to the

imputed non-DeepSEA SNPs contained in our dataset, these predicted functional DeepSEA SNPs were enriched for TSS and enhancer regions and depleted for quiescent regions, supporting their relevance in regulatory processes (see Figure 4). Compared to DeepSEA SNPs overall, DeepSEA SNPs within the 3 different best models also showed distinct enrichment or depletion patterns. Similar to GxE VMRs, likely functional GxE SNPs also showed a relative depletion in TSS regions while G+E SNPs showed enrichment in genic enhancers. Overall, both the VMRs as well as the associated functional SNPs appear to be in distinct regulatory regions, depending on their best model. In addition, GxE functional SNP and tagCpGs were located farther apart than SNP/tagCpG pairs within G or G+E models (see Supplementary Figure 5B), supporting a more long-range type of regulation in GxE interactions on molecular traits as compared to all genes; a similar relationship has been reported previously for GxE with regard to gene expression in *C. elegans*^{51,52}. SNPs associated with differences in gene expression but also DNA methylation have consistently been shown to be enriched among SNPs associated with common disorders in GWAS^{21,24,26,53}. The functional genetic variants that were within G, GxE or G+E models predicting variable DNA methylation were even enriched in GWAS association results (beyond the baseline enrichment of DeepSea SNPs per se). The fact that such enrichment was observed for not only G and G+E SNPs, with strong main genetic effects, but also for GxE SNPs, with smaller to sometimes no main genetic effect on DNA methylation underscores the importance of also including SNPs within GxE models in the functional annotation of GWAS. A detailed catalogue of meQTLs that are responsive to environmental factors could support a better pathophysiological understanding of diseases for which risk is shaped by a combination of environment and genetic factors.

Finally, we want to note the limitations of this study. First, we restricted our analyses to specific DNA methylation array contents that are inherently biased as compared to genome-wide bisulfite sequencing, for example. In addition, we restricted our analysis to VMRs, which also limits the generalizability of the findings, but also has advantages. Ong and Holbrooke⁵⁴ showed that this approach increases statistical power. Furthermore, VMRs are enriched for enhancers and transcription factor binding sites, overlap with GWAS hits⁵⁵ and are associated with gene-expression of nearby genes at these sites⁵⁶. VMRs in this study presented with intermediate methylation levels which have been shown to be enriched in regions of regulatory function, like enhancers, exons and DNase I hypersensitivity sites⁵⁷. Hence, the effects of genotypes on DNA methylation levels in VMRs might be higher as compared to less variable CpG-sites. In addition, genotypes are measured with much less error as compared to environmental factors which may also reduce the overall explained variance in large cohorts.

Second, it has been reported that different cell types display different patterns of DNA methylation⁵⁵. Therefore, the most variable CpG-sites may also include those that reflect differences in cord blood cell type proportions. To address this issue, all analyses were corrected for estimated cell proportions to the best of our current availability, so that differences in cell type proportion likely do not account for all of the observed effects. However, only replication in specific cell types will be able to truly assess the proportion of VMRs influenced by this.

Third, we used the AIC as main criterion for model fit³⁷ which is equivalent to a penalized likelihood-function. There are a variety of other model selection criteria⁵⁸ and choosing between these is an ongoing debate which also depends on the underlying research question. We decided to use the AIC as one of our main aims was to compare our results with the study of Teh et al.²⁹

in which this criterion was applied and as this method maybe more powerful for detecting GxE than for example model selection criteria based on lowest p-values.

Fourth, all reported interactions are statistical interactions and limited to a *cis* window around the CpG-site. Further experiments are required to assess whether these would also reflect biological/mechanistic interactions. Much larger cohorts will be needed to assess potential *trans* effects. Additional inclusion of further covariates such as maternal smoking or maternal age may further modify the effects of specific Es but is beyond the scope of this manuscript.

Fifth, as summarized in Table 1, results presented are based on cohorts which differ in ethnicity, assessed phenotypes, methylation and SNP arrays, processing pipelines and sample sizes. While all these factors may contribute to differences in the proportions of models across the cohorts, it also suggests that our findings are quite robust to these methodological issues.

Finally, our analyses are restricted to DNA methylation in neonatal blood and to pregnancy environments. Whether similar conclusions can be drawn for methylation levels assessed at a later developmental stage needs to be investigated.

We tested whether genotype, a combination of different prenatal environmental factors and the additive or the multiplicative interactive effects of both mainly influence VMRs in the newborn's epigenome. Our results show that G in combination with E are the best predictors of variance in DNA methylation. This highlights the importance of including both individual genetic differences as well as environmental phenotypes into epigenetic studies and also the importance of improving our ability to identify environmental associations. Our data also support the disease relevance of variants predicting DNA methylation together with the environment beyond main meQTL effects, and the view that there are functional differences of additive and interactive effects of genes and environment on DNA methylation. Improved understanding of these

functional differences may also yield novel insights into pathophysiological mechanisms of common non-communicable diseases, as risk for all of these disorders is driven by both genetic and environmental factors.

Methods

The PREDO cohort

The Prediction and Prevention of Preeclampsia and Intrauterine Growth Restriction (PREDO) Study is a longitudinal multicenter pregnancy cohort study of Finnish women and their singleton children born alive between 2006-2010³⁰. We recruited 1,079 pregnant women, of whom 969 had one or more and 110 had none of the known clinical risk factors for preeclampsia and intrauterine growth restriction. The recruitment took place when these women attended the first ultrasound screening at 12+0-13+6 weeks+days of gestation in one of the ten hospital maternity clinics participating in the study. The cohort profile³⁰ contains details of the study design and inclusion criteria.

Ethics

The study protocol was approved by the Ethical Committees of the Helsinki and Uusimaa Hospital District and by the participating hospitals. A written informed consent was obtained from all women.

Maternal characteristics

We tested 10 different maternal environments:

Depressive symptoms

503 Starting from 12+0-13+6 gestational weeks+days pregnant women filled in the 20 item Center
504 for Epidemiological Studies Depression Scale (CES-D) ⁵⁹ for depressive symptoms in the past 7
505 days. They filled in the CES-D scale biweekly until 38+0-39+6 weeks+days of gestation or
506 delivery. We used the mean-value across all the CES-D measurements.

507 *Symptoms of anxiety*

508 At 12+0-13+6 weeks+days of gestation, women filled in the 20 item Spielberger's State Trait
509 Anxiety Inventory (STAI) ⁶⁰ for anxiety symptoms in the past 7 days. They filled in the STAI
510 scale biweekly until 38+0-39+6 weeks+days of gestation or delivery. We used the mean-value
511 across all these measurements.

512 *Betamethasone*

513 Antenatal betamethasone treatment (yes/no) was derived from the hospital records and the
514 Finnish Medical Birth Register (MBR).

515 *Delivery method*

516 Mode of delivery (vaginal delivery vs. caesarean section) was derived from patient records and
517 MBR.

518 *Parity*

519 Parity (number of previous pregnancies leading to childbirth) at the start of present pregnancy
520 was derived from the hospital records and the MBR.

521 *Maternal age*

522 Maternal age at delivery (years) was derived from the hospital records and the MBR.

523 *Pre-pregnancy BMI*

Maternal pre-pregnancy BMI (kg/m^2), calculated from measurements weight and height verified at the first antenatal clinic visit at 8+4 (SD 1+3) gestational week was derived from the hospital records and the MBR.

Hypertension

Hypertension was defined as any hypertensive disorder including gestational hypertension, chronic hypertension and preeclampsia against normotension. Gestational hypertension was defined as systolic/diastolic blood pressure $\geq 140/90$ mm Hg on ≥ 2 occasions at least 4 h apart in a woman who was normotensive before 20th week of gestation. Preeclampsia was defined as systolic/diastolic blood pressure $\geq 140/90$ mm Hg on ≥ 2 occasions at least 4 h apart after 20th week of gestation and proteinuria ≥ 300 mg/24 h. Chronic hypertension was defined as systolic/diastolic blood pressure $\geq 140/90$ mm Hg on ≥ 2 occasions at least 4 h apart before 20th gestational week or medication for hypertension before 20 weeks of gestation.

Gestational diabetes and oral glucose tolerance test (OGTT)

Gestational diabetes was defined as fasting, 1h or 2h plasma glucose during a 75g oral glucose tolerance test ≥ 5.1 , ≥ 10.0 and/or ≥ 8.5 mmol/L, respectively, that emerged or was first identified during pregnancy. We took the area under the curve from the three measurements as a single measure for the OGTT itself.

Genotyping and Imputation

Genotyping was performed on Illumina Human Omni Express Exome Arrays containing 964,193 SNPs. Only markers with a call rate of at least 98%, a minor allele frequency of at least 1% and a p-value for deviation from Hardy-Weinberg-Equilibrium $> 1.0 \times 10^{-6}$ were kept in the analysis. After QC, 587,290 SNPs were available.

546 In total, 996 cord blood samples were genotyped. Samples with a call rate below 98% (n=11)
547 were removed.

548 Any pair of samples with IBD estimates > 0.125 was checked for relatedness. As we corrected
549 for admixture in our analyses using MDS-components (see Supplemental Figure 10), these
550 samples were kept except for one pair which could not be resolved. From this pair we excluded
551 one sample from further analysis. Individuals showing discrepancies between phenotypic and
552 genotypic sex (n=1) were removed. We also checked for heterozygosity outliers but found none.
553 983 participants were available in the final dataset.

554 Before imputation, AT and CG SNPs were removed. Imputation was performed using shapeit2
555 (https://mathgen.stats.ox.ac.uk/genetics_software/shapeit/shapeit.html) and impute2
556 (https://mathgen.stats.ox.ac.uk/impute/impute_v2.html). Chromosomal and base pair positions
557 were updated to the 1000 Genomes Phase 3 reference set, allele strands were flipped where
558 necessary.

559 After imputation, we reran quality control, filtering out SNPs with an info score < 0.8 , a minor
560 allele frequency below 1% and a deviation from HWE with a p-value $< 1.0 \times 10^{-6}$.

561 This resulted in a dataset of 9,402,991 SNPs. After conversion into best guessed genotypes
562 using a probability threshold of 90%, we performed another round of QC (using SNP-call rate of
563 least 98%, a MAF of at least 1% and a p-value threshold for HWE of 1.0×10^{-6}), after which
564 7,314,737 SNPs remained for the analysis.

565 For the evaluation of which model best explained the methylation sites, we pruned the dataset
566 using a threshold of r^2 of 0.2 and a window-size of 50 SNPs with an overlap of 5 SNPs. The
567 final, pruned dataset contained 788,156 SNPs. 36,241 of these variants were DeepSea variants
568 (see Methods below).

569 *Methylation*

570 Cord blood samples were run on Illumina 450k Methylation arrays. The quality control pipeline
571 was set up using the R-package *minfi* ⁶¹ (<https://www.r-project.org>). Three samples were
572 excluded as they were outliers in the median intensities. Furthermore, 20 samples showed
573 discordance between phenotypic sex and estimated sex and were excluded. Nine samples were
574 contaminated with maternal DNA according to the method suggested by Morin et al. ⁶² and were
575 also removed.

576 Methylation beta-values were normalized using the *funnorm* function ⁶³. After normalization,
577 two batches, i.e., slide and well, were significantly associated and were removed iteratively using
578 the *Combat* function ⁶⁴ in the *sva* package ⁶⁵.

579 We excluded any probes on chromosome X or Y, probes containing SNPs and cross-hybridizing
580 probes according to Chen et al. ⁵³ and Price et al ⁶⁶. Furthermore, any CpGs with a detection p-
581 value > 0.01 in at least 25% of the samples were excluded.

582 The final dataset contained 428,619 CpGs and 822 participants. For 817 of these, also genotypes
583 were available.

584 An additional 161 cord blood samples were run on Illumina EPIC Methylation arrays.

585 Three samples were excluded as they were outliers in the median intensities. Three samples
586 showed discordance between phenotypic sex and estimated sex and were excluded. Three
587 samples were contaminated with maternal DNA and were also removed ⁶².

588 Methylation beta-values were normalized using the *funnorm* function ⁶³ in the R-package *minfi*
589 ⁶¹. Three samples showed density artefacts after normalization and were removed from further
590 analysis. We excluded any probes on chromosome X or Y, probes containing SNPs and cross-
591 hybridizing probes according to Chen et al. ⁵³, Price et al. ⁶⁶ and McCartney et al. ⁶⁷.

Furthermore, any CpGs with a detection p-value > 0.01 in at least 25% of the samples were excluded. The final dataset contains 812,987 CpGs and 149 samples. After normalization no significant batches were identified. For 146 of these samples, genotypic data was also available. Cord blood cell counts were estimated for seven cell types (nucleated red blood cells, granulocytes, monocytes, natural killer cells, B cells, CD4(+)T cells, and CD8(+)T cells) using the method of Bakulski et al.⁶⁸ which is incorporated in the R-package *minfi*⁶¹.

Identification of VMRs (variable methylated regions)

The VMR approach was described by Ong and Holbrook⁵⁴. We chose all 42,862 CpGs with a MAD score greater than the 90th percentile. For each CpG-site, the MAD (median absolute deviation) is defined as the median of the absolute deviations from each individual's methylation beta-value at this CpG-site to the CpG's median. A candidate VMR region was defined as at least two spatially contiguous probes which were at most 1kb apart of each other. This resulted in 3,982 VMRs in the 450K samples and in 8,547 VMRs in the EPIC sample. The CpG with the highest MAD scores was chosen as representative of the whole VMR in the statistical analysis.

Drakenstein cohort

Details on this cohort and the assessed phenotypes can be found in^{34,35}. The birth cohort design recruits pregnant women attending one of two primary health care clinics in the Drakenstein sub-district of the Cape Winelands, Western Cape, South Africa – Mbekweni (serving a black African population) and TC Newman (serving a mixed ancestry population). Consenting mothers were enrolled during pregnancy, and mother–child dyads are followed longitudinally until children reach at least 5 years of age. Mothers are asked to request that the father of the index

pregnancy attend a single antenatal study visit where possible. Follow-up visits for mother–child dyads take place at the two primary health care clinics and at Paarl Hospital.

Pregnant women were eligible to participate if they were 18 years or older, were accessing one of the two primary health care clinics for antenatal care, had no intention to move out of the district within the following year, and provided signed written informed consent. Participants were enrolled between 20 and 28 weeks’ gestation, upon presenting for antenatal care visit. In addition, consenting fathers of the index pregnancy when available were enrolled in the study and attended a single antenatal study visit.

Ethics

The study was approved by the Faculty of Health Sciences, Human Research Ethics Committee, University of Cape Town (401/2009), by Stellenbosch University (N12/02/0002), and by the Western Cape Provincial Health Research committee (2011RP45). All participants provided written informed consent.

Maternal characteristics

After providing consent, participants were asked to complete a battery of self-report and clinician-administered measures at a number of antenatal and postnatal study visits. All assessed phenotypes are described in detail in ³⁴. Here, we give a short outline on the phenotypes which were used in our analysis. Maternal parity was obtained from the antenatal record; maternal age was from the date of birth as recorded on the mothers’ national identity document. The mode of delivery was ascertained by direct observation of the birth by a member of the study team as all births occurred at Paarl hospital. The SRQ-20 ⁶⁹ is a WHO-endorsed measure of psychological distress consisting of 20 items which assess non-psychotic symptoms, including symptoms of depressive and anxiety disorders. Each item is scored according to whether the participant

responds in the affirmative (scored as 1) or negative (scored as 0) to the presence of a symptom. Individual items are summed to generate a total score. The Beck Depression Inventory (BDI-II) is a widely-used and reliable measure of depressive symptoms⁷⁰. The BDI-II comprises 21 items, each of which assesses the severity of a symptom of major depression. Each item is assessed on a severity scale ranging from 0 (absence of symptoms) to 3 (severe, often with functional impairment). A total score is then obtained by summing individual item responses, with a higher score indicative of more severe depressive symptoms.

Smoking was assessed using The Alcohol, Smoking and Substance Involvement Screening Test (ASSIST)⁷¹, a tool that was developed by the WHO to detect and manage substance use among people attending primary health care services. The tool assesses substance use and substance-related risk across 10 categories (tobacco, alcohol, cannabis, cocaine, amphetamine-type stimulants, inhalants, sedatives/sleeping pills, hallucinogens, opioids, and other substances), as well as enquiring about a history of intravenous drug use. Total scores are obtained for each substance by summing individual item responses, with a higher score indicative of greater risk for substance-related health problems.

Hypertension was assessed by blood pressure measured antenatally.

Genotyping and Imputation

Genotyping in DCHS was performed using the Illumina PsychArray for those samples with 450k data, or the Illumina GSA for those samples with EPIC DNA methylation data (Illumina, San Diego, USA). For both array types, QC and imputation was the same; first, raw data was imported into Genome Studio and exported into R for QC. SNPs were filtered out if they had a tenth percentile GC score below 0.2 or an average GC score below 0.1, for a total of 140 SNPs

removed. Phasing was performed using shapeit, and imputation was performed using impute2 with 1000 Genomes Phase 1 reference data. After imputation, we used qctool to filter out SNPs with an info score <0.8 or out of Hardy-Weinberg equilibrium. All SNPs with MAF <1% were removed.

As after imputation, only 5,286 DeepSEA variants were available for those samples genotyped on the PsychArray and only 4,049 for those samples genotyped on the GSAchip , we performed LD-pruning based on a threshold of r^2 of 0.2 and a window-size of 50 SNPs with an overlap of 5 SNPs. This resulted in 162,292 SNPs (PsychArray) and 176,553 SNPs (GSAchip).

Methylation

We performed basic quality control on data generated by either the 450k or EPIC arrays using Illumina's Genome Studio software for background subtraction and colour correction. Data was filtered to remove CpGs with high detection p values, those on the X or Y chromosome, or with previously identified poor performance. 450k data was normalized using SWAN and EPIC data using BMIQ, and both used ComBat to correct for chip (both), and row (450k only). Details for DNA methylation measurements and quality control have been published ⁶². The final analysis was performed with 107 samples with methylation levels from the 450k array and 151 with methylation levels assessed on the EPIC array and available genotypes. Neonatal blood cell counts were estimated for seven cell types: nucleated red blood cells, granulocytes, monocytes, natural killer cells, B cells, CD4(+)T cells, and CD8(+)T cells ⁶⁸.

VMRs

We identified 6,072 candidate VMRs in DCHS I and 10,005 candidate VMRs in DCHS II.

The UCI cohort

Mothers and children were part of an ongoing, longitudinal study, conducted at the University of California, Irvine (UCI), for which mothers were recruited during the first trimester of pregnancy³¹⁻³³. All women had singleton, intrauterine pregnancies. Women were not eligible for study participation if they met the following criteria: corticosteroids, or illicit drugs during pregnancy (verified by urinary cotinine and drug toxicology). Exclusion criteria for the newborn were preterm birth (i.e., less than 34 weeks of gestational age at birth), as well as any congenital, genetic, or neurologic disorders at birth.

Ethics

The UCI institutional review board approved all study procedures and all participants provided written informed consent.

Maternal Characteristics

Maternal sociodemographic characteristics (age, parity) were obtained via a standardized structured interview at the first pregnancy visit. Maternal pre-pregnancy BMI (weight kg/height m²) was computed based on pre-pregnancy weight abstracted from the medical record, and maternal height was measured at the research laboratory during the first pregnancy visit.

Obstetric risk conditions during pregnancy, including presence of gestational diabetes and hypertension, and delivery mode were abstracted from the medical record. At each pregnancy visit the Center for Epidemiological Studies Depression Scale⁵⁹ and the State scale from the State-Trait Anxiety Inventory⁶⁰ were administered. For individuals with <3 missing items on any scale at any time point, the mean responses for that scale were calculated and then multiplied by the total number of items in the respective scale, to generate total scale scores that are comparable to those generated from participants without any missing data. We used the average depression and anxiety score throughout pregnancy in the calculations. Maternal smoking during

pregnancy was determined by maternal self-report and verified by measurement of urinary cotinine concentration. Urinary cotinine was assayed in maternal samples collected at each trimester using the Nicotine/COT(Cotinine)/Tobacco Drug Test Urine Cassette (<http://www.meditests.com/nicuintescas.html>), which involves transferring 4 drops of room temperature urine into the well of the cassette, and employs a cutoff for COT presence of 200ng/ml. Endorsement of smoking or detection of urinary COT in any trimester was coded as 1, and absence of evidence for smoking in any trimester coded as 0.

Genotyping

Genomic DNA was extracted from heel prick blood samples and used for all genomic analysis. Genotyping was performed on Illumina Human Omni Express (24 v1.1) Arrays containing 713,014 SNPs. All samples had a high call rate (above 97%). SNPs with a minor allele frequency >5% and a p-value for deviation from Hardy-Weinberg-Equilibrium $> 1.0 \times 10^{-25}$ were retained for analysis. After QC, 602,807 SNPs were available.

Imputation

Before imputation, chromosomal and base pair positions were updated to the Haplotype Reference Consortium (r1.1) reference set, allele strands were flipped where necessary. Phasing was performed using EAGLE2 (<https://data.broadinstitute.org/alkesgroup/Eagle/>) and imputation was performed using PBWT (<https://github.com/VertebrateResequencing/pbwt>). Imputed SNPs with an info score < 0.8 , duplicates and ambiguous SNPs were removed resulting in 21,341,980 SNPs. All SNPs with MAF < 0.01 were removed. Of the remaining SNPs, 19,530 were DeepSEA variants.

DNA Methylation

DNAm analysis using the Infinium Illumina MethylationEPIC BeadChip (Illumina, Inc., San Diego, CA) was performed according to the manufacturer's guidelines in using genomic DNA derived from neonatal heel prick samples. Quality Control carried out in *minfi*⁶¹. No outliers were detected in the median intensities of methylated and unmethylated channels. All samples had a high call rate of at least 95% and their predicted sex was the same as the phenotypic sex. We removed CpGs with a high detection value ($p < 0.0001$), probes missing >3 beads in >5% of the cohort, in addition to non-specific/cross-hybridizing and SNP probes^{66,67}. Methylation beta-values were normalized using functional normalization (*funnorm*)⁶³. We also iteratively adjusted the data for relevant technical factors, i.e. array row, experimental batch and sample plate, using *Combat*⁶⁴. The final dataset contained 768,910 CpGs. Neonatal blood cell counts were estimated for seven cell types: nucleated red blood cells, granulocytes, monocytes, natural killer cells, B cells, CD4(+)T cells, and CD8(+)T cells⁶⁸. The final dataset contained 121 samples with available genotypes and methylation values.

VMRs

Applying the same procedure as for PREDO I and PREDO II, we identified 9,525 candidate VMRs in the ICU cohort.

MoBa cohort

Participants represent two subsets of mother-offspring pairs from the national Norwegian Mother and Child Cohort Study (MoBa)⁷². MoBa is a prospective population-based pregnancy cohort study conducted by the Norwegian Institute of Public Health. The years of birth for MoBa participants ranged from 1999-2009. MoBa mothers provided written informed consent. Each subset is referred to here as MoBa1 and MoBa2. MoBa1 is a subset of a larger study within

MoBa that included a cohort random sample and cases of asthma at age three years⁷³. We previously reported an association between maternal smoking during pregnancy and differential DNA methylation in MoBa1 newborns⁷⁴. We subsequently measured DNA methylation in additional newborns (MoBa2) in the same laboratory (Illumina, San Diego, CA)¹¹. MoBa2 included cohort random sample plus cases of asthma at age seven years and non-asthmatic controls. Years of birth were 2002-2004 for children in MoBa1, 2000-2005 for MoBa2.

Ethics

The establishment and data collection in MoBa obtained a license from the Norwegian Data Inspectorate and approval from The Regional Committee for Medical Research Ethics. Both studies were approved by the Regional Committee for Ethics in Medical Research, Norway. In addition, MoBa1 and MoBa2 were approved by the Institutional Review Board of the National Institute of Environmental Health Sciences, USA.

Maternal characteristics

To replicate specific GxE and G+E from PREDO I, we focused on those characteristics which were available in both cohorts: maternal age, pre-pregnancy BMI and hypertension. Within MoBa, the questionnaires at weeks 17 and 30 include general background information as well as details on previous and present health problems and exposures. The birth record from the Medical Birth Registry of Norway⁷⁵ which includes maternal health during pregnancy as well as procedures around birth and pregnancy outcomes, is integrated in the MoBa database.

Genotyping and Imputation

DNA was extracted from the MoBa biobank and genotyped on the Illumina HumanExomeCore platform. The genotypes were called with GenomeStudio software. Phasing and imputation were done using shapeit2 (https://mathgen.stats.ox.ac.uk/genetics_software/shapeit/shapeit.html) and

impute2 (https://mathgen.stats.ox.ac.uk/impute/impute_v2.html) with the thousand genomes phase 3 reference panel for the European population. Variants with a imputation score of less than 0.8 and with a minor allele frequency below 1% were filtered out.

Methylation

Details of the DNA methylation measurements and quality control for the MoBa1 participants were previously described³⁶ and the same protocol was implemented for the MoBa2 participants. Briefly, at birth, umbilical cord blood samples were collected and frozen at birth at -80°C. All biological material was obtained from the Biobank of the MoBa study³⁶. Bisulfite conversion was performed using the EZ-96 DNA Methylation kit (Zymo Research Corporation, Irvine, CA) and DNA methylation was measured at 485,577 CpGs in cord blood using Illumina's Infinium HumanMethylation450 BeadChip⁷⁶. Raw intensity (.idat) files were handled in R using the *minfi* package to calculate the methylation level at each CpG as the beta-value ($\beta = \text{intensity of the methylated allele (M)} / (\text{intensity of the unmethylated allele (U)} + \text{intensity of the methylated allele (M)} + 100))$) and the data was exported for quality control and processing. Control probes (N=65) and probes on X (N=11 230) and Y (N=416) chromosomes were excluded in both datasets. Remaining CpGs missing > 10% of methylation data were also removed (N=20 in MoBa1, none in MoBa2). Samples indicated by Illumina to have failed or have an average detection p value across all probes < 0.05 (N=49 MoBa1, N=35 MoBa2) and samples with gender mismatch (N=13 MoBa1, N=8 MoBa2) were also removed. For MoBa1 and MoBa2, we accounted for the two different probe designs by applying the intra-array normalization strategy Beta Mixture Quantile dilation (BMIQ)⁷⁷. The Empirical Bayes method via *ComBat* was applied separately in MoBa1 and MoBa2 for batch correction using the *sva* package in R⁶⁵. After quality control exclusions, the sample sizes were 1,068 for MoBa1 and 685 for MoBa2.

After QC, the total number of samples was 1,732, with 1,592 overlapping with the methylation samples. Specific G+E and GxE associations were calculated in the combined dataset of MoBa1 and MoBa2, while VMR analysis was conducted in MoBa1 only.

Regression analysis

Linear regression analysis was conducted using the *lm* function in R 3.3.1 (<https://www.r-project.org>). We included the child's sex, gestational age, seven estimated cell counts as well as the first two (PREDO I and PREDO II), first three (UCI) and first five (DCHS I and II) principal components of the MDS analysis on the genotypes in the model. The corresponding plot of the first ten MDS-components in PREDO is depicted in Figure S4. SNP genotypes were recoded into a count of 0, 1 or 2 representing the number of minor allele copies. For each VMR site, we tested SNPs located in a 1MB window up- and downstream of the specific site. In PREDO and UCI, we restricted the analysis to DeepSEA variants while we used the pruned SNP-set in DCHS.

For each VMR, we tested four models:

(1) Methylation at tagCpG ~ covariates + environment

(2) Methylation at tagCpG ~ covariates + SNP

(3) Methylation at tagCpG ~ covariates + SNP + environment

(4) Methylation at tagCpG ~ covariates + SNP + environment + SNP x environment

In model (1) we included all ten different environments, in model (2) all DeepSEA cis SNPs and in models (3) and (4) all possible environment-cis-SNP combinations. Please also see Figure 1.

819 For each model, the AIC, Akaike's information criterion ³⁷ was calculated and the model with
820 the lowest AIC was chosen as the best model. The AIC was obtained using the *AIC* function in
821 R 3.3.1 (<https://www.r-project.org>).

822 P-values were obtained from the summary function and adjusted for the number of tested Es (E
823 model), of tested cis SNPs (G model) or of tested cis SNP-environment combinations (G+E/GxE
824 model) using Bonferroni-correction. Afterwards, we used FDR to correct for all tested tagCpGs
825 (all models) using *p.adjust* in R.

826

827 *Enrichment analyses*

828 With regard to enrichment for VMRs, CpG-site within VMRs were compared to all other CpG-
829 sites on the 450K array located in non-VMR-regions. With regard to enrichment for VMRs best
830 explained by G, G+E or GxE, tagCpGs best explained by the specific model were compared to
831 tagCpGs best explained by any of the other models. For enrichment tests for DeepSEA SNPs,
832 non-DeepSEA SNPs present in our dataset were used as comparison group. Enrichment tests
833 were performed based on a hyper-geometric test, i.e. a Fisher-test. The significance levels was
834 set at $p < 0.05$.

835 With regard to enrichment for GWAS hits, DeepSEA variants were matched to GWAS variants
836 based on chromosome and position (hg19). To check for enrichment for nominal significant
837 GWAS hits, the full summary statistics were derived from the respective publication.

838 Histone ChIP-seq peaks from Roadmap Epigenomics project for blood and embryonic stem cells
839 were downloaded from
840 <http://egg2.wustl.edu/roadmap/data/byFileType/peaks/consolidated/broadPeak/>.

841 The pre-processed consolidated broad peaks from the uniform processing pipeline of the
842 Roadmap project were used.

843

844 *Genomic annotation mapping*

845 CpG sites were mapped to the genome location according to Illumina's annotation using the R-
846 package *minfi*.

847

848 *DeepSEA Analysis*

849 Pretrained DeepSEA model was downloaded from:

850 <http://deepsea.princeton.edu/media/code/deepsea.v0.94.tar.gz> and variant files in VCF format are
851 used for producing e-values. VCF files were first split into smaller files each containing one
852 million variants and the model was run using the command line on a server with a NVIDIA Titan
853 X GPU card.

854 We reran our models using only DeepSEA variants which had been identified by the algorithm
855 of Zhou and Troyanskaya³⁸. This method predicts functionality of a SNP based on the DNA-
856 sequence. We included all 212,210 variants with a functional significance e-value below 5×10^{-05} .
857 The e-values represent the significance of the regulatory impact of given variants compared to
858 one million random variants.

859

860 *Random-effects meta-analysis*

861 GxE and G+E result for PREDO and for MoBa were meta-analysed using a random-effects
862 model in the R-package *rmeta*. Replication was defined as DeepSEA-tagCpG-environment
863 combinations showing the same effect direction in both cohorts, presenting with smaller p-values

as for PREDO alone and with a FDR-corrected p-value (across all combinations tested in the meta-analysis) below 0.05.

Data availability

The datasets analyzed during the current study are not publicly available. However, an interested researcher can obtain a de-identified dataset after approval from the PREDO Study Board. Data requests may be subject to further review by the national register authority and by the ethical committees. Any requests for data use should be addressed to the PREDO Study Board (predo.study@helsinki.fi) or individual researchers. The summary statistics of the best models for PREDO I are accessible at: <https://doi.org/10.6084/m9.figshare.8074964>.

For access to the UCI cohort, please contact claudia.buss@charite.de , for access to DCHS please contact Heather.Zar@uct.ac.za, for MoBa access please apply for data access at <https://www.fih.no>

Acknowledgements

We want to thank Susanne Sauer and Maik Ködel for their technical assistance. We thank all mothers who took part in the on-going PREDO study. We are grateful to all the families in Norway who participate in the on-going MoBa cohort study. We thank the Drakenstein Child Health Study staff, and the clinical and administrative staff of the Western Cape Government Department of Health at Paarl Hospital and at the clinics for support of the Study. We also thank our collaborators and students. Finally, we thank all mothers and children enrolled in the Drakenstein Child Health Study. We thank the research participants and employees of 23andMe, Inc. for their contribution to this study.

887

888 ***Author's contributions***

889 DC and EBB conceived the analyses.

890 JL, MLP, EH, EK, HL, PMV, RRM and KR conceptualized and planned the PREDO study and
891 collected the data.

892 CMP, WN, SH and SJL conceptualized and planned the MoBa study and collected the data.

893 CB, SE, PWD, KJOD conceptualized and planned the UCI study and collected the data.

894 DTSL and JLM performed the DNA methylation and genotyping arrays for the UCI and DCH
895 studies.

896 DJS, NK, HJZ designed and undertook the DCHS; MJM, MSK, KCK were involved in testing
897 and analysis of epigenetic data; SD was involved in testing and analysis of genetic data.

898 DC, GE, CMP and MJJ ran the statistical analysis.

899 NSM, IK and FJT co-supervised statistical analysis.

900 DC and EBB wrote the manuscript with contributions from GE, SJL, CMP, KR, JL.

901 DC, JL, KR, and EB interpreted the results.

902 All authors contributed to and approved the final version of the manuscript.

903

904 ***Competing interests***

905 DC, GE, JL, CMP, MLP, EH, EK, HL, PMV, RMR, WN, SH, SJL, KJOD, EG, MJM, SE, PDW,
906 CB, MJJ, DTSL, JLMI, MSK, NK, HJZ, KCK, SD, DJS, IK, NSM, FJT, KR have no competing
907 interests. EBB is co-inventor on the following patent applications: FKBP5: a novel target for
908 antidepressant therapy. European Patent# EP 1687443 B1; Polymorphisms in ABCB1 associated
909 with a lack of clinical response to medicaments. United States Patent # 8030033; Means and

methods for diagnosing predisposition for treatment emergent suicidal ideation (TESI). European application number: 08016477.5 International application number: PCT/EP2009/061575.

Funding

This work was supported by the Academy of Finland (EK, HL, KR, JL); University of Helsinki Research Funds (JL, MLP,HL), British Heart Foundation (RMR); Tommy's (RMR); European Commission (EK, KR, Horizon 2020 Award SC1-2016-RTD-733280 RECAP); NorFace DIAL (EK, KR PremLife); Foundation for Pediatric Research (EK); Juho Vainio Foundation (EK); Novo Nordisk Foundation (EK); Signe and Ane Gyllenberg Foundation (EK, KR); Sigrid Jusélius Foundation (EK); Finnish Medical Foundation (HL); Jane and Aatos Erkko Foundation (HL); Päivikki and Sakari Sohlberg Foundation (HL, PMV); the Clinical Graduate school in Pediatrics and Obstetrics/Gynaecology in University of Helsinki (PMV). The Norwegian Mother and Child Cohort Study is supported by the Norwegian Ministry of Health and Care Services and the Ministry of Education and Research, NIH/NIEHS (contract no N01-ES-75558), NIH/NINDS (grant no.1 U01 NS 047537-01 and grant no.2 U01 NS 047537-06A1). For this work, MoBa 1 and 2 were supported by the Intramural Research Program of the NIH, National Institute of Environmental Health Sciences (Z01-ES-49019) and the Norwegian Research Council/BIOBANK (grant no 221097). This work was also partly supported by the Research Council of Norway through its Centres of Excellence funding scheme, project number 262700. The Drakenstein Child Health Study is supported by the Bill and Melinda Gates Foundation (OPP 1017641); with additional support for this work from the Eunice Kennedy Shriver National Institute of Child Health and Human Development of the National Institutes of Health (NICHD) under Award Number R21HD085849; and the Fogarty International Center (FIC). The content

is solely the responsibility of the authors and does not necessarily represent the official views of the National Institutes of Health. Additional support for HJZ, DJS and NK, and for research reported in this publication was by the South African Medical Research Council (SAMRC); NK receives support from the SAMRC under a Self-Initiated Research Grant. The views and opinions expressed are those of the authors and do not necessarily represent the official views of the SAMRC.

This work was also funded by the German Federal Ministry of Education and Research through the Research Consortium Integrated Network IntegraMent (grant 01ZX1314H) under the auspices of the e:Med Programme (NSM).

The UCI cohort was supported by a European Research Area Network (ERA Net) Neuron grant (01EW1407A, CB) and National Institutes of Health grant (R01 HD-060628, CB) as well as NIH grant R01 MH-105538 (PDW).

This work was also funded by the Canadian Institute for Advanced Research, Child and Brain Development Program, Toronto, ON, Canada (KJOD).

Figures and figure legends

Figure 1: Flow diagram of VMR analysis

Figure 2: VMR-analysis in pruned PREDO I dataset

A: Percentage of models (G, E, GxE or G+E) with the lowest AIC explaining variable DNA methylation using the PREDO I dataset with pruned SNPs.

B: Distribution of the different types of prenatal environment included in the E model with the lowest AIC (right), in the combinations yielding the best model GxE (middle), or the best model G+E models (left). To increase readability all counts < 3% have been omitted.

C: DeltaAIC, i.e., the difference in AIC, between best model and next best model, stratified by the best model. Y-axis denotes the delta AIC and the X-axis the different models. The median is depicted by a black line, the rectangle spans the first quartile to the third quartile, whiskers above

and below the box show the location of minimum and maximum beta-values. P-values are based on Wilcoxon-tests.

Figure 3: VMR-analysis in DeepSEA annotated SNPs in PREDO I dataset.

A: Percentage of models (G, E, GxE or G+E) with the lowest AIC explaining variable DNA methylation using the PREDO I dataset with DeepSEA annotated SNPs.

B: Distribution of the locations of all VMRs and tagVMRs with best model E, G, G+E and GxE on the 450k array using only DeepSEA variants in relationship to CpG-Islands based on the Illumina 450K annotation.

C: Distribution of gene-centric locations of all VMRs and tagVMRs with best model E, G, G+E and GxE on the 450k array using only DeepSEA variants.

Figure 4: Functional annotation of VMR-mapping in DeepSEA annotated SNPs in PREDO I dataset

A: Histone mark enrichment for all VMRs. The Y-axis denotes the fold enrichment/depletion as compared to no-VMRs. Blue bars indicate significant enrichment/depletion, grey bars non-significant differences based on Fisher-tests.

B: Histone mark enrichment for tagVMRs with best model E, G, G+E and GxE relative to all VMRs. Green color indicates depletion, red color indicates enrichment. Thick black lines around the rectangles indicate significant enrichment/depletion based on Fisher-tests.

C: Histone mark enrichment for all DeepSEA variants in the dataset. Blue bars indicate significant enrichment/depletion based on Fisher-tests.

D: Histone mark enrichment for all DeepSEA variants involved in models where either G, G+E or GxE is the best model as compared to all tested DeepSEA variants. Green color indicates depletion, red color indicates enrichment. Thick black lines around the rectangles indicate significant enrichment/depletion based on Fisher-tests.

Figure 5: VMR-analysis in PREDO I and replication datasets

Percentage of models (G, E, GxE or G+E) with the lowest AIC explaining variable DNA methylation in PREDO I (450K), DCHS I (450K), PREDO II (EPIC), UCI (EPIC) and DCHS II (EPIC)

Figure 6: Consistency of best models across cohorts

Percentage of consistent best models in overlapping tag CpGs of PREDO I (450K), DCHS I (450K), PREDO II (EPIC), UCI (EPIC) and DCHS II (EPIC). Overlapping VMRs included significantly more CpGs as compared to all VMRs ($p < 2.2 \times 10^{-16}$, Wilcoxon-test, mean=4.43).

Figure 7: Enrichment of DeepSEA variants for GWAS associations

A: Enrichment for nominal significant GWAS associations for all tested DeepSEA variants and their LD proxies for GWAS for ADHD (attention deficit hyperactivity disorder), ASD (autism spectrum disorder), BMI (body-mass index), BP (bipolar disorder), CrossDisorder, IBD (inflammatory bowel disease), MDD (major depressive disorder), SCZ (schizophrenia) and T2D (Type 2 diabetes). The Y-axis denotes the fold enrichment with regard to non-DeepSEA variants. Blue bars indicate significant enrichment/depletion based on Fisher-tests.

B: Enrichment for nominal significant GWAS hits for DeepSEA variants and their LD proxies involved in best models with G, G+E or GxE as compared to all tested DeepSEA variants. Green color indicates depletion, red color indicates enrichment. Thick black lines around the rectangles indicate significant enrichment/depletion based on Fisher-tests.

Bibliography

- 1 Roseboom, T., de Rooij, S. & Painter, R. The Dutch famine and its long-term consequences for adult health. *Early Hum Dev* **82**, 485-491, doi:10.1016/j.earlhumdev.2006.07.001 (2006).
- 2 Barker, D. J., Osmond, C., Forsen, T. J., Kajantie, E. & Eriksson, J. G. Trajectories of growth among children who have coronary events as adults. *N Engl J Med* **353**, 1802-1809, doi:10.1056/NEJMoa044160 (2005).
- 3 Hovi, P. *et al.* Glucose regulation in young adults with very low birth weight. *N Engl J Med* **356**, 2053-2063, doi:10.1056/NEJMoa067187 (2007).
- 4 Hillier, T. A. *et al.* Childhood obesity and metabolic imprinting: the ongoing effects of maternal hyperglycemia. *Diabetes Care* **30**, 2287-2292, doi:10.2337/dc06-2361 (2007).
- 5 Dancause, K. N. *et al.* Prenatal stress due to a natural disaster predicts adiposity in childhood: the Iowa Flood Study. *J Obes* **2015**, 570541, doi:10.1155/2015/570541 (2015).
- 6 Lahti, M. *et al.* Maternal Depressive Symptoms During and After Pregnancy and Psychiatric Problems in Children. *J Am Acad Child Adolesc Psychiatry* **56**, 30-39 e37, doi:10.1016/j.jaac.2016.10.007 (2017).
- 7 Bronson, S. L. & Bale, T. L. The Placenta as a Mediator of Stress Effects on Neurodevelopmental Reprogramming. *Neuropsychopharmacology* **41**, 207-218, doi:10.1038/npp.2015.231 (2016).
- 8 Schwarze, C. E. *et al.* Prenatal adversity: a risk factor in borderline personality disorder? *Psychol Med* **43**, 1279-1291, doi:10.1017/S0033291712002140 (2013).
- 9 Entringer, S., Buss, C. & Wadhwa, P. D. Prenatal stress, development, health and disease risk: A psychobiological perspective-2015 Curt Richter Award Paper. *Psychoneuroendocrinology* **62**, 366-375, doi:10.1016/j.psyneuen.2015.08.019 (2015).
- 10 Gutierrez-Arcelus, M. *et al.* Passive and active DNA methylation and the interplay with genetic variation in gene regulation. *Elife* **2**, e00523, doi:10.7554/eLife.00523 (2013).
- 11 Joubert, B. R. *et al.* DNA Methylation in Newborns and Maternal Smoking in Pregnancy: Genome-wide Consortium Meta-analysis. *Am J Hum Genet* **98**, 680-696, doi:10.1016/j.ajhg.2016.02.019 (2016).
- 12 Sharp, G. C. *et al.* Maternal BMI at the start of pregnancy and offspring epigenome-wide DNA methylation: findings from the pregnancy and childhood epigenetics (PACE) consortium. *Hum Mol Genet* **26**, 4067-4085, doi:10.1093/hmg/ddx290 (2017).
- 13 Girchenko, P. *et al.* Associations between maternal risk factors of adverse pregnancy and birth outcomes and the offspring epigenetic clock of gestational age at birth. *Clin Epigenetics* **9**, 49, doi:10.1186/s13148-017-0349-z (2017).
- 14 Rijlaarsdam, J. *et al.* An epigenome-wide association meta-analysis of prenatal maternal stress in neonates: A model approach for replication. *Epigenetics* **11**, 140-149, doi:10.1080/15592294.2016.1145329 (2016).
- 15 Sosnowski, D. W., Booth, C., York, T. P., Amstadter, A. B. & Kliewer, W. Maternal prenatal stress and infant DNA methylation: A systematic review. *Dev Psychobiol* **60**, 127-139, doi:10.1002/dev.21604 (2018).
- 16 Bauer, T. *et al.* Environment-induced epigenetic reprogramming in genomic regulatory elements in smoking mothers and their children. *Mol Syst Biol* **12**, 861, doi:10.15252/msb.20156520 (2016).

1079 17 Sharp, G. C. *et al.* Maternal pre-pregnancy BMI and gestational weight gain, offspring
1080 DNA methylation and later offspring adiposity: findings from the Avon Longitudinal Study
1081 of Parents and Children. *Int J Epidemiol* **44**, 1288-1304, doi:10.1093/ije/dyv042 (2015).
1082 18 Lin, X. *et al.* Developmental pathways to adiposity begin before birth and are
1083 influenced by genotype, prenatal environment and epigenome. *BMC Med* **15**, 50,
1084 doi:10.1186/s12916-017-0800-1 (2017).
1085 19 Cecil, C. A. *et al.* DNA methylation and substance-use risk: a prospective, genome-
1086 wide study spanning gestation to adolescence. *Transl Psychiatry* **6**, e976,
1087 doi:10.1038/tp.2016.247 (2016).
1088 20 Gibbs, J. R. *et al.* Abundant quantitative trait loci exist for DNA methylation and gene
1089 expression in human brain. *PLoS Genet* **6**, e1000952, doi:10.1371/journal.pgen.1000952
1090 (2010).
1091 21 Gaunt, T. R. *et al.* Systematic identification of genetic influences on methylation
1092 across the human life course. *Genome Biol* **17**, 61, doi:10.1186/s13059-016-0926-z (2016).
1093 22 McClay, J. L. *et al.* High density methylation QTL analysis in human blood via next-
1094 generation sequencing of the methylated genomic DNA fraction. *Genome Biol* **16**, 291,
1095 doi:10.1186/s13059-015-0842-7 (2015).
1096 23 Chen, L. *et al.* Genetic Drivers of Epigenetic and Transcriptional Variation in Human
1097 Immune Cells. *Cell* **167**, 1398-1414 e1324, doi:10.1016/j.cell.2016.10.026 (2016).
1098 24 Hannon, E., Weedon, M., Bray, N., O'Donovan, M. & Mill, J. Pleiotropic Effects of Trait-
1099 Associated Genetic Variation on DNA Methylation: Utility for Refining GWAS Loci. *Am J Hum*
1100 *Genet* **100**, 954-959, doi:10.1016/j.ajhg.2017.04.013 (2017).
1101 25 Pierce, B. L. *et al.* Co-occurring expression and methylation QTLs allow detection of
1102 common causal variants and shared biological mechanisms. *Nat Commun* **9**, 804,
1103 doi:10.1038/s41467-018-03209-9 (2018).
1104 26 Cheung, W. A. *et al.* Functional variation in allelic methylomes underscores a strong
1105 genetic contribution and reveals novel epigenetic alterations in the human epigenome.
1106 *Genome Biol* **18**, 50, doi:10.1186/s13059-017-1173-7 (2017).
1107 27 Gluckman, P. D., Hanson, M. A., Cooper, C. & Thornburg, K. L. Effect of in utero and
1108 early-life conditions on adult health and disease. *N Engl J Med* **359**, 61-73,
1109 doi:10.1056/NEJMra0708473 (2008).
1110 28 Klengel, T. *et al.* Allele-specific FKBP5 DNA demethylation mediates gene-childhood
1111 trauma interactions. *Nat Neurosci* **16**, 33-41, doi:10.1038/nn.3275 (2013).
1112 29 Teh, A. L. *et al.* The effect of genotype and in utero environment on interindividual
1113 variation in neonate DNA methylomes. *Genome Res* **24**, 1064-1074,
1114 doi:10.1101/gr.171439.113 (2014).
1115 30 Girchenko, P. *et al.* Prediction and Prevention of Preeclampsia and Intrauterine
1116 Growth Restriction (PREDO) study. *International journal of epidemiology*,
1117 doi:10.1093/ije/dyw154 (2016).
1118 31 Graham, A. M. *et al.* Maternal Systemic Interleukin-6 During Pregnancy Is Associated
1119 With Newborn Amygdala Phenotypes and Subsequent Behavior at 2 Years of Age. *Biol*
1120 *Psychiatry* **83**, 109-119, doi:10.1016/j.biopsych.2017.05.027 (2018).
1121 32 Moog, N. K. *et al.* Intergenerational Effect of Maternal Exposure to Childhood
1122 Maltreatment on Newborn Brain Anatomy. *Biol Psychiatry* **83**, 120-127,
1123 doi:10.1016/j.biopsych.2017.07.009 (2018).

1124 33 Entringer, S. *et al.* Maternal Cortisol During Pregnancy and Infant Adiposity: A
1125 Prospective Investigation. *J Clin Endocrinol Metab* **102**, 1366-1374, doi:10.1210/jc.2016-
1126 3025 (2017).

1127 34 Stein, D. J. *et al.* Investigating the psychosocial determinants of child health in Africa:
1128 The Drakenstein Child Health Study. *J Neurosci Methods* **252**, 27-35,
1129 doi:10.1016/j.jneumeth.2015.03.016 (2015).

1130 35 Zar, H. J., Barnett, W., Myer, L., Stein, D. J. & Nicol, M. P. Investigating the early-life
1131 determinants of illness in Africa: the Drakenstein Child Health Study. *Thorax* **70**, 592-594,
1132 doi:10.1136/thoraxjnl-2014-206242 (2015).

1133 36 Ronningen, K. S. *et al.* The biobank of the Norwegian Mother and Child Cohort Study:
1134 a resource for the next 100 years. *Eur J Epidemiol* **21**, 619-625, doi:10.1007/s10654-006-
1135 9041-x (2006).

1136 37 Akaike, H. in *Proceedings of the Second International Symposium on Information*
1137 *Theory* (ed. 267-281 (Akademai Kiado, 1973
1138).

1139 38 Zhou, J. & Troyanskaya, O. G. Predicting effects of noncoding variants with deep
1140 learning-based sequence model. *Nat Methods* **12**, 931-934, doi:10.1038/nmeth.3547
1141 (2015).

1142 39 Consortium, E. P. The ENCODE (ENCyclopedia Of DNA Elements) Project. *Science*
1143 **306**, 636-640, doi:10.1126/science.1105136 (2004).

1144 40 Autism Spectrum Disorders Working Group of The Psychiatric Genomics, C. Meta-
1145 analysis of GWAS of over 16,000 individuals with autism spectrum disorder highlights a
1146 novel locus at 10q24.32 and a significant overlap with schizophrenia. *Mol Autism* **8**, 21,
1147 doi:10.1186/s13229-017-0137-9 (2017).

1148 41 Demontis, D. *et al.* Discovery of the first genome-wide significant risk loci for
1149 attention deficit/hyperactivity disorder. *Nat Genet* **51**, 63-75, doi:10.1038/s41588-018-
1150 0269-7 (2019).

1151 42 Psychiatric, G. C. B. D. W. G. Large-scale genome-wide association analysis of bipolar
1152 disorder identifies a new susceptibility locus near ODZ4. *Nat Genet* **43**, 977-983,
1153 doi:10.1038/ng.943 (2011).

1154 43 Wray, N. R. *et al.* Genome-wide association analyses identify 44 risk variants and
1155 refine the genetic architecture of major depression. *Nat Genet* **50**, 668-681,
1156 doi:10.1038/s41588-018-0090-3 (2018).

1157 44 Schizophrenia Working Group of the Psychiatric Genomics, C. Biological insights
1158 from 108 schizophrenia-associated genetic loci. *Nature* **511**, 421-427,
1159 doi:10.1038/nature13595 (2014).

1160 45 Cross-Disorder Group of the Psychiatric Genomics, C. Identification of risk loci with
1161 shared effects on five major psychiatric disorders: a genome-wide analysis. *Lancet* **381**,
1162 1371-1379, doi:10.1016/S0140-6736(12)62129-1 (2013).

1163 46 Liu, J. Z. *et al.* Association analyses identify 38 susceptibility loci for inflammatory
1164 bowel disease and highlight shared genetic risk across populations. *Nat Genet* **47**, 979-986,
1165 doi:10.1038/ng.3359 (2015).

1166 47 Morris, A. P. *et al.* Large-scale association analysis provides insights into the genetic
1167 architecture and pathophysiology of type 2 diabetes. *Nat Genet* **44**, 981-990,
1168 doi:10.1038/ng.2383 (2012).

1169 48 Horikoshi, M. *et al.* Discovery and Fine-Mapping of Glycaemic and Obesity-Related
 1170 Trait Loci Using High-Density Imputation. *PLoS Genet* **11**, e1005230,
 1171 doi:10.1371/journal.pgen.1005230 (2015).
 1172 49 Sandoval, J. *et al.* Validation of a DNA methylation microarray for 450,000 CpG sites
 1173 in the human genome. *Epigenetics* **6**, 692-702 (2011).
 1174 50 Mehta, D. *et al.* Childhood maltreatment is associated with distinct genomic and
 1175 epigenetic profiles in posttraumatic stress disorder. *Proc Natl Acad Sci U S A* **110**, 8302-
 1176 8307, doi:10.1073/pnas.1217750110 (2013).
 1177 51 Grishkevich, V., Yanai, I. The genomic determinants of genotype \times environment
 1178 interactions in gene expression. *Trends in Genetics* **29**, 479-487 (2013).
 1179 52 Grishkevich, V. *et al.* A genomic bias for genotype-environment interactions in *C.*
 1180 *elegans*. *Mol Syst Biol* **8**, 587, doi:10.1038/msb.2012.19 (2012).
 1181 53 Chen, Y. A. *et al.* Discovery of cross-reactive probes and polymorphic CpGs in the
 1182 Illumina Infinium HumanMethylation450 microarray. *Epigenetics* **8**, 203-209,
 1183 doi:10.4161/epi.23470 (2013).
 1184 54 Ong, M. L. & Holbrook, J. D. Novel region discovery method for Infinium 450K DNA
 1185 methylation data reveals changes associated with aging in muscle and neuronal pathways.
 1186 *Aging Cell* **13**, 142-155, doi:10.1111/accel.12159 (2014).
 1187 55 Gu, J. *et al.* Mapping of Variable DNA Methylation Across Multiple Cell Types Defines
 1188 a Dynamic Regulatory Landscape of the Human Genome. *G3 (Bethesda)* **6**, 973-986,
 1189 doi:10.1534/g3.115.025437 (2016).
 1190 56 Feinberg, A. P. & Irizarry, R. A. Evolution in health and medicine Sackler colloquium:
 1191 Stochastic epigenetic variation as a driving force of development, evolutionary adaptation,
 1192 and disease. *Proc Natl Acad Sci U S A* **107 Suppl 1**, 1757-1764,
 1193 doi:10.1073/pnas.0906183107 (2010).
 1194 57 Elliott, G. *et al.* Intermediate DNA methylation is a conserved signature of genome
 1195 regulation. *Nat Commun* **6**, 6363, doi:10.1038/ncomms7363 (2015).
 1196 58 Zhang, P. Inference after variable selection in linear regression models. *Biometrika*
 1197 **79**, 741-746 (1992).
 1198 59 Radloff, L. S. The CES-D Scale: A Self-Report Depression Scale for Research in the
 1199 General Population. *Appl Psychol Meas* **1**, 385-401 (1977).
 1200 60 Spielberger, C. D. *State-Trait Anxiety Inventory: Bibliography*. 2nd Edition edn,
 1201 (Consulting Psychologists Press, 1989).
 1202 61 Aryee, M. J. *et al.* Minfi: a flexible and comprehensive Bioconductor package for the
 1203 analysis of Infinium DNA methylation microarrays. *Bioinformatics* **30**, 1363-1369,
 1204 doi:10.1093/bioinformatics/btu049 (2014).
 1205 62 Morin, A. M. *et al.* Maternal blood contamination of collected cord blood can be
 1206 identified using DNA methylation at three CpGs. *Clin Epigenetics* **9**, 75,
 1207 doi:10.1186/s13148-017-0370-2 (2017).
 1208 63 Fortin, J. P. *et al.* Functional normalization of 450k methylation array data improves
 1209 replication in large cancer studies. *Genome Biol* **15**, 503, doi:10.1186/s13059-014-0503-2
 1210 (2014).
 1211 64 Johnson, W. E., Li, C. & Rabinovic, A. Adjusting batch effects in microarray expression
 1212 data using empirical Bayes methods. *Biostatistics* **8**, 118-127,
 1213 doi:10.1093/biostatistics/kxj037 (2007).

1214 65 Leek, J. T., Johnson, W. E., Parker, H. S., Jaffe, A. E. & Storey, J. D. The sva package for
 1215 removing batch effects and other unwanted variation in high-throughput experiments.
 1216 *Bioinformatics* **28**, 882-883, doi:10.1093/bioinformatics/bts034 (2012).
 1217 66 Price, M. E. *et al.* Additional annotation enhances potential for biologically-relevant
 1218 analysis of the Illumina Infinium HumanMethylation450 BeadChip array. *Epigenetics*
 1219 *Chromatin* **6**, 4, doi:10.1186/1756-8935-6-4 (2013).
 1220 67 McCartney, D. L. *et al.* Identification of polymorphic and off-target probe binding
 1221 sites on the Illumina Infinium MethylationEPIC BeadChip. *Genom Data* **9**, 22-24,
 1222 doi:10.1016/j.gdata.2016.05.012 (2016).
 1223 68 Bakulski, K. M. *et al.* DNA methylation of cord blood cell types: Applications for
 1224 mixed cell birth studies. *Epigenetics* **11**, 354-362, doi:10.1080/15592294.2016.1161875
 1225 (2016).
 1226 69 van der Westhuizen, C., Wyatt, G., Williams, J. K., Stein, D. J. & Sorsdahl, K. Validation
 1227 of the Self Reporting Questionnaire 20-Item (SRQ-20) for Use in a Low- and Middle-Income
 1228 Country Emergency Centre Setting. *Int J Ment Health Addict* **14**, 37-48,
 1229 doi:10.1007/s11469-015-9566-x (2016).
 1230 70 Beck, A. T., Ward, C. H., Mendelson, M., Mock, J. & Erbaugh, J. An inventory for
 1231 measuring depression. *Arch Gen Psychiatry* **4**, 561-571 (1961).
 1232 71 Group, W. A. W. The Alcohol, Smoking and Substance Involvement Screening Test
 1233 (ASSIST): development, reliability and feasibility. *Addiction* **97**, 1183-1194 (2002).
 1234 72 Magnus, P. *et al.* Cohort Profile Update: The Norwegian Mother and Child Cohort
 1235 Study (MoBa). *Int J Epidemiol* **45**, 382-388, doi:10.1093/ije/dyw029 (2016).
 1236 73 Haberg, S. E. *et al.* Maternal folate levels in pregnancy and asthma in children at age
 1237 3 years. *J Allergy Clin Immunol* **127**, 262-264, 264 e261, doi:10.1016/j.jaci.2010.10.004
 1238 (2011).
 1239 74 Joubert, B. R. *et al.* 450K epigenome-wide scan identifies differential DNA
 1240 methylation in newborns related to maternal smoking during pregnancy. *Environ Health*
 1241 *Perspect* **120**, 1425-1431, doi:10.1289/ehp.1205412 (2012).
 1242 75 Irgens, L. M. The Medical Birth Registry of Norway. Epidemiological research and
 1243 surveillance throughout 30 years. *Acta Obstet Gynecol Scand* **79**, 435-439 (2000).
 1244 76 Bibikova, M. *et al.* High density DNA methylation array with single CpG site
 1245 resolution. *Genomics* **98**, 288-295, doi:10.1016/j.ygeno.2011.07.007 (2011).
 1246 77 Teschendorff, A. E. *et al.* A beta-mixture quantile normalization method for
 1247 correcting probe design bias in Illumina Infinium 450 k DNA methylation data.
 1248 *Bioinformatics* **29**, 189-196, doi:10.1093/bioinformatics/bts680 (2013).
 1249

1250 **Listing of Psychiatric Genomics Consortium Members**

1251 Major Depressive Disorder Working Group

Naomi R Wray* 1, 2
 Stephan Ripke* 3, 4, 5
 Manuel Mattheisen* 6, 7, 8, 9

Maciej Trzaskowski* 1
 Enda M Byrne 1
 Abdel Abdellaoui 10

Mark J Adams 11
 Esben Agerbo 9, 12, 13
 Tracy M Air 14
 Till F M Andlauer 15, 16
 Silviu-Alin Bacanu 17
 Marie Bækvad-Hansen 9, 18
 Aartjan T F Beekman 19
 Tim B Bigdeli 17, 20
 Elisabeth B Binder 15, 21
 Douglas H R Blackwood 11
 Julien Bryois 22
 Henriette N Buttenschøn 8, 9, 23
 Jonas Bybjerg-Grauholm 9, 18
 Na Cai 24, 25
 Enrique Castelao 26
 Jane Hvarregaard Christensen 7, 8, 9
 Toni-Kim Clarke 11
 Jonathan R I Coleman 27
 Lucía Colodro-Conde 28
 Baptiste Couvy-Duchesne 2, 29
 Nick Craddock 30
 Gregory E Crawford 31, 32
 Gail Davies 33
 Ian J Deary 33
 Franziska Degenhardt 34, 35
 Eske M Derks 28
 Nese Direk 36, 37
 Conor V Dolan 10
 Erin C Dunn 38, 39, 40
 Thalia C Eley 27
 Valentina Escott-Price 41
 Farnush Farhadi Hassan Kiadeh 42
 Hilary K Finucane 43, 44
 Andreas J Forstner 34, 35, 45, 46
 Josef Frank 47
 Héléna A Gaspar 27
 Michael Gill 48
 Fernando S Goes 49
 Scott D Gordon 28
 Jakob Grove 7, 8, 9, 50
 Lynsey S Hall 11, 51
 Christine Søholm Hansen 9, 18
 Thomas F Hansen 52, 53, 54
 Stefan Herms 34, 35, 46
 Ian B Hickie 55
 Per Hoffmann 34, 35, 46
 Georg Homuth 56
 Carsten Horn 57
 Jouke-Jan Hottenga 10
 David M Hougaard 9, 18
 Marcus Ising 58
 Rick Jansen 19, 19
 Ian Jones 59
 Lisa A Jones 60
 Eric Jorgenson 61
 James A Knowles 62
 Isaac S Kohane 63, 64, 65
 Julia Kraft 4
 Warren W. Kretschmar 66
 Jesper Krogh 67
 Zoltán Kutalik 68, 69
 Yihan Li 66
 Penelope A Lind 28
 Donald J MacIntyre 70, 71
 Dean F MacKinnon 49
 Robert M Maier 2
 Wolfgang Maier 72
 Jonathan Marchini 73
 Hamdi Mbarek 10
 Patrick McGrath 74
 Peter McGuffin 27
 Sarah E Medland 28
 Divya Mehta 2, 75
 Christel M Middeldorp 10, 76, 77
 Evelin Mihailov 78
 Yuri Milaneschi 19, 19
 Lili Milani 78
 Francis M Mondimore 49
 Grant W Montgomery 1
 Sara Mostafavi 79, 80
 Niamh Mullins 27
 Matthias Nauck 81, 82
 Bernard Ng 80
 Michel G Nivard 10
 Dale R Nyholt 83
 Paul F O'Reilly 27
 Hogni Oskarsson 84
 Michael J Owen 59
 Jodie N Painter 28
 Carsten Bøcker Pedersen 9, 12, 13
 Marianne Giørtz Pedersen 9, 12, 13
 Roseann E. Peterson 17, 85

Erik Pettersson 22
 Wouter J Peyrot 19
 Giorgio Pistis 26
 Danielle Posthuma 86, 87
 Jorge A Quiroz 88
 Per Qvist 7, 8, 9
 John P Rice 89
 Brien P. Riley 17
 Margarita Rivera 27, 90
 Saira Saeed Mirza 36
 Robert Schoevers 91
 Eva C Schulte 92, 93
 Ling Shen 61
 Jianxin Shi 94
 Stanley I Shyn 95
 Engilbert Sigurdsson 96
 Grant C B Sinnamon 97
 Johannes H Smit 19
 Daniel J Smith 98
 Hreinn Stefansson 99
 Stacy Steinberg 99
 Fabian Streit 47
 Jana Strohmaier 47
 Katherine E Tansey 100
 Henning Teismann 101
 Alexander Teumer 102
 Wesley Thompson 9, 53, 103, 104
 Pippa A Thomson 105
 Thorgeir E Thorgeirsson 99
 Matthew Traylor 106
 Jens Treutlein 47
 Vassily Trubetskoy 4
 André G Uitterlinden 107
 Daniel Umbricht 108
 Sandra Van der Auwera 109
 Albert M van Hemert 110
 Alexander Viktorin 22
 Peter M Visscher 1, 2
 Yunpeng Wang 9, 53, 104
 Bradley T. Webb 111
 Shantel Marie Weinsheimer 9, 53
 Jürgen Wellmann 101
 Gonneke Willemsen 10
 Stephanie H Witt 47
 Yang Wu 1
 Hualin S Xi 112

Jian Yang 2, 113
 Futao Zhang 1
 Volker Arolt 114
 Bernhard T Baune 14
 Klaus Berger 101
 Dorret I Boomsma 10
 Sven Cichon 34, 46, 115, 116
 Udo Dannlowski 114
 EJC de Geus 10, 117
 J Raymond DePaulo 49
 Enrico Domenici 118
 Katharina Domschke 119
 Tõnu Esko 5, 78
 Hans J Grabe 109
 Steven P Hamilton 120
 Caroline Hayward 121
 Andrew C Heath 89
 Kenneth S Kendler 17
 Stefan Kloiber 58, 122, 123
 Glyn Lewis 124
 Qingqin S Li 125
 Susanne Lucae 58
 Pamela AF Madden 89
 Patrik K Magnusson 22
 Nicholas G Martin 28
 Andrew M McIntosh 11, 33
 Andres Metspalu 78, 126
 Ole Mors 9, 127
 Preben Bo Mortensen 8, 9, 12, 13
 Bertram Müller-Myhsok 15, 16, 128
 Merete Nordentoft 9, 129
 Markus M Nöthen 34, 35
 Michael C O'Donovan 59
 Sara A Paciga 130
 Nancy L Pedersen 22
 Brenda WJH Penninx 19
 Roy H Perlis 38, 131
 David J Porteous 105
 James B Potash 132
 Martin Preisig 26
 Marcella Rietschel 47
 Catherine Schaefer 61
 Thomas G Schulze 47, 93, 133, 134, 135
 Jordan W Smoller 38, 39, 40
 Kari Stefansson 99, 136
 Henning Tiemeier 36, 137, 138

Rudolf Uher 139
Henry Völzke 102
Myrna M Weissman 74, 140
Thomas Werge 9, 53, 141
Cathryn M Lewis* 27, 142
Douglas F Levinson* 143
Gerome Breen* 27, 144
Anders D Børglum* 7, 8, 9
Patrick F Sullivan* 22, 145, 146

- 1
- 2
- 3 1. Institute for Molecular Bioscience, The University of Queensland, Brisbane, QLD, AU
- 4 2. Queensland Brain Institute, The University of Queensland, Brisbane, QLD, AU
- 5 3. Analytic and Translational Genetics Unit, Massachusetts General Hospital, Boston, MA,
- 6 US
- 7 4. Department of Psychiatry and Psychotherapy, Universitätsmedizin Berlin Campus Charité
- 8 Mitte, Berlin, DE
- 9 5. Medical and Population Genetics, Broad Institute, Cambridge, MA, US
- 10 6. Centre for Psychiatry Research, Department of Clinical Neuroscience, Karolinska
- 11 Institutet, Stockholm, SE
- 12 7. Department of Biomedicine, Aarhus University, Aarhus, DK
- 13 8. iSEQ, Centre for Integrative Sequencing, Aarhus University, Aarhus, DK
- 14 9. iPSYCH, The Lundbeck Foundation Initiative for Integrative Psychiatric Research,, DK
- 15 10. Dept of Biological Psychology & EMGO+ Institute for Health and Care Research, Vrije
- 16 Universiteit Amsterdam, Amsterdam, NL
- 17 11. Division of Psychiatry, University of Edinburgh, Edinburgh, GB
- 18 12. Centre for Integrated Register-based Research, Aarhus University, Aarhus, DK
- 19 13. National Centre for Register-Based Research, Aarhus University, Aarhus, DK
- 20 14. Discipline of Psychiatry, University of Adelaide, Adelaide, SA, AU
- 21 15. Department of Translational Research in Psychiatry, Max Planck Institute of Psychiatry,
- 22 Munich, DE
- 23 16. Munich Cluster for Systems Neurology (SyNergy), Munich, DE
- 24 17. Department of Psychiatry, Virginia Commonwealth University, Richmond, VA, US
- 25 18. Center for Neonatal Screening, Department for Congenital Disorders, Statens Serum
- 26 Institut, Copenhagen, DK
- 27 19. Department of Psychiatry, Vrije Universiteit Medical Center and GGZ inGeest,
- 28 Amsterdam, NL
- 29 20. Virginia Institute for Psychiatric and Behavior Genetics, Richmond, VA, US
- 30 21. Department of Psychiatry and Behavioral Sciences, Emory University School of
- 31 Medicine, Atlanta, GA, US
- 32 22. Department of Medical Epidemiology and Biostatistics, Karolinska Institutet, Stockholm,
- 33 SE
- 34 23. Department of Clinical Medicine, Translational Neuropsychiatry Unit, Aarhus University,
- 35 Aarhus, DK
- 36 24. Human Genetics, Wellcome Trust Sanger Institute, Cambridge, GB
- 37 25. Statistical genomics and systems genetics, European Bioinformatics Institute (EMBL-
- 38 EBI), Cambridge, GB
- 39 26. Department of Psychiatry, University Hospital of Lausanne, Prilly, Vaud, CH
- 40 27. Social Genetic and Developmental Psychiatry Centre, King's College London, London,
- 41 GB
- 42 28. Genetics and Computational Biology, QIMR Berghofer Medical Research Institute,
- 43 Brisbane, QLD, AU
- 44 29. Centre for Advanced Imaging, The University of Queensland, Brisbane, QLD, AU
- 45 30. Psychological Medicine, Cardiff University, Cardiff, GB
- 46 31. Center for Genomic and Computational Biology, Duke University, Durham, NC, US
- 47 32. Department of Pediatrics, Division of Medical Genetics, Duke University, Durham, NC,
- 48 US
- 49 33. Centre for Cognitive Ageing and Cognitive Epidemiology, University of Edinburgh,
- 50 Edinburgh, GB
- 51 34. Institute of Human Genetics, University of Bonn, Bonn, DE

- 52 35. Life&Brain Center, Department of Genomics, University of Bonn, Bonn, DE
- 53 36. Epidemiology, Erasmus MC, Rotterdam, Zuid-Holland, NL
- 54 37. Psychiatry, Dokuz Eylul University School Of Medicine, Izmir, TR
- 55 38. Department of Psychiatry, Massachusetts General Hospital, Boston, MA, US
- 56 39. Psychiatric and Neurodevelopmental Genetics Unit (PNGU), Massachusetts General
- 57 Hospital, Boston, MA, US
- 58 40. Stanley Center for Psychiatric Research, Broad Institute, Cambridge, MA, US
- 59 41. Neuroscience and Mental Health, Cardiff University, Cardiff, GB
- 60 42. Bioinformatics, University of British Columbia, Vancouver, BC, CA
- 61 43. Department of Epidemiology, Harvard T.H. Chan School of Public Health, Boston, MA,
- 62 US
- 63 44. Department of Mathematics, Massachusetts Institute of Technology, Cambridge, MA, US
- 64 45. Department of Psychiatry (UPK), University of Basel, Basel, CH
- 65 46. Human Genomics Research Group, Department of Biomedicine, University of Basel,
- 66 Basel, CH
- 67 47. Department of Genetic Epidemiology in Psychiatry, Central Institute of Mental Health,
- 68 Medical Faculty Mannheim, Heidelberg University, Mannheim, Baden-Württemberg, DE
- 69 48. Department of Psychiatry, Trinity College Dublin, Dublin, IE
- 70 49. Psychiatry & Behavioral Sciences, Johns Hopkins University, Baltimore, MD, US
- 71 50. Bioinformatics Research Centre, Aarhus University, Aarhus, DK
- 72 51. Institute of Genetic Medicine, Newcastle University, Newcastle upon Tyne, GB
- 73 52. Danish Headache Centre, Department of Neurology, Rigshospitalet, Glostrup, DK
- 74 53. Institute of Biological Psychiatry, Mental Health Center Sct. Hans, Mental Health
- 75 Services Capital Region of Denmark, Copenhagen, DK
- 76 54. iPSYCH, The Lundbeck Foundation Initiative for Psychiatric Research, Copenhagen, DK
- 77 55. Brain and Mind Centre, University of Sydney, Sydney, NSW, AU
- 78 56. Interfaculty Institute for Genetics and Functional Genomics, Department of Functional
- 79 Genomics, University Medicine and Ernst Moritz Arndt University Greifswald, Greifswald,
- 80 Mecklenburg-Vorpommern, DE
- 81 57. Roche Pharmaceutical Research and Early Development, Pharmaceutical Sciences, Roche
- 82 Innovation Center Basel, F. Hoffmann-La Roche Ltd, Basel, CH
- 83 58. Max Planck Institute of Psychiatry, Munich, DE
- 84 59. MRC Centre for Neuropsychiatric Genetics and Genomics, Cardiff University, Cardiff,
- 85 GB
- 86 60. Department of Psychological Medicine, University of Worcester, Worcester, GB
- 87 61. Division of Research, Kaiser Permanente Northern California, Oakland, CA, US
- 88 62. Psychiatry & The Behavioral Sciences, University of Southern California, Los Angeles,
- 89 CA, US
- 90 63. Department of Biomedical Informatics, Harvard Medical School, Boston, MA, US
- 91 64. Department of Medicine, Brigham and Women's Hospital, Boston, MA, US
- 92 65. Informatics Program, Boston Children's Hospital, Boston, MA, US
- 93 66. Wellcome Trust Centre for Human Genetics, University of Oxford, Oxford, GB
- 94 67. Department of Endocrinology at Herlev University Hospital, University of Copenhagen,
- 95 Copenhagen, DK
- 96 68. Institute of Social and Preventive Medicine (IUMSP), University Hospital of Lausanne,
- 97 Lausanne, VD, CH
- 98 69. Swiss Institute of Bioinformatics, Lausanne, VD, CH
- 99 70. Division of Psychiatry, Centre for Clinical Brain Sciences, University of Edinburgh,
- 100 Edinburgh, GB
- 101 71. Mental Health, NHS 24, Glasgow, GB
- 102 72. Department of Psychiatry and Psychotherapy, University of Bonn, Bonn, DE

103 73. Statistics, University of Oxford, Oxford, GB
 104 74. Psychiatry, Columbia University College of Physicians and Surgeons, New York, NY, US
 105 75. School of Psychology and Counseling, Queensland University of Technology, Brisbane,
 106 QLD, AU
 107 76. Child and Youth Mental Health Service, Children's Health Queensland Hospital and
 108 Health Service, South Brisbane, QLD, AU
 109 77. Child Health Research Centre, University of Queensland, Brisbane, QLD, AU
 110 78. Estonian Genome Center, University of Tartu, Tartu, EE
 111 79. Medical Genetics, University of British Columbia, Vancouver, BC, CA
 112 80. Statistics, University of British Columbia, Vancouver, BC, CA
 113 81. DZHK (German Centre for Cardiovascular Research), Partner Site Greifswald, University
 114 Medicine, University Medicine Greifswald, Greifswald, Mecklenburg-Vorpommern, DE
 115 82. Institute of Clinical Chemistry and Laboratory Medicine, University Medicine
 116 Greifswald, Greifswald, Mecklenburg-Vorpommern, DE
 117 83. Institute of Health and Biomedical Innovation, Queensland University of Technology,
 118 Brisbane, QLD, AU
 119 84. Humus, Reykjavik, IS
 120 85. Virginia Institute for Psychiatric & Behavioral Genetics, Virginia Commonwealth
 121 University, Richmond, VA, US
 122 86. Clinical Genetics, Vrije Universiteit Medical Center, Amsterdam, NL
 123 87. Complex Trait Genetics, Vrije Universiteit Amsterdam, Amsterdam, NL
 124 88. Solid Biosciences, Boston, MA, US
 125 89. Department of Psychiatry, Washington University in Saint Louis School of Medicine,
 126 Saint Louis, MO, US
 127 90. Department of Biochemistry and Molecular Biology II, Institute of Neurosciences, Center
 128 for Biomedical Research, University of Granada, Granada, ES
 129 91. Department of Psychiatry, University of Groningen, University Medical Center
 130 Groningen, Groningen, NL
 131 92. Department of Psychiatry and Psychotherapy, Medical Center of the University of
 132 Munich, Campus Innenstadt, Munich, DE
 133 93. Institute of Psychiatric Phenomics and Genomics (IPPG), Medical Center of the
 134 University of Munich, Campus Innenstadt, Munich, DE
 135 94. Division of Cancer Epidemiology and Genetics, National Cancer Institute, Bethesda, MD,
 136 US
 137 95. Behavioral Health Services, Kaiser Permanente Washington, Seattle, WA, US
 138 96. Faculty of Medicine, Department of Psychiatry, University of Iceland, Reykjavik, IS
 139 97. School of Medicine and Dentistry, James Cook University, Townsville, QLD, AU
 140 98. Institute of Health and Wellbeing, University of Glasgow, Glasgow, GB
 141 99. deCODE Genetics / Amgen, Reykjavik, IS
 142 100. College of Biomedical and Life Sciences, Cardiff University, Cardiff, GB
 143 101. Institute of Epidemiology and Social Medicine, University of Münster, Münster,
 144 Nordrhein-Westfalen, DE
 145 102. Institute for Community Medicine, University Medicine Greifswald, Greifswald,
 146 Mecklenburg-Vorpommern, DE
 147 103. Department of Psychiatry, University of California, San Diego, San Diego, CA, US
 148 104. KG Jebsen Centre for Psychosis Research, Norway Division of Mental Health and
 149 Addiction, Oslo University Hospital, Oslo, NO
 150 105. Medical Genetics Section, CGEM, IGMM, University of Edinburgh, Edinburgh, GB
 151 106. Clinical Neurosciences, University of Cambridge, Cambridge, GB
 152 107. Internal Medicine, Erasmus MC, Rotterdam, Zuid-Holland, NL

153 108. Roche Pharmaceutical Research and Early Development, Neuroscience, Ophthalmology
 154 and Rare Diseases Discovery & Translational Medicine Area, Roche Innovation Center Basel,
 155 F. Hoffmann-La Roche Ltd, Basel, CH
 156 109. Department of Psychiatry and Psychotherapy, University Medicine Greifswald,
 157 Greifswald, Mecklenburg-Vorpommern, DE
 158 110. Department of Psychiatry, Leiden University Medical Center, Leiden, NL
 159 111. Virginia Institute for Psychiatric & Behavioral Genetics, Virginia Commonwealth
 160 University, Richmond, VA, US
 161 112. Computational Sciences Center of Emphasis, Pfizer Global Research and Development,
 162 Cambridge, MA, US
 163 113. Institute for Molecular Bioscience; Queensland Brain Institute, The University of
 164 Queensland, Brisbane, QLD, AU
 165 114. Department of Psychiatry, University of Münster, Münster, Nordrhein-Westfalen, DE
 166 115. Institute of Medical Genetics and Pathology, University Hospital Basel, University of
 167 Basel, Basel, CH
 168 116. Institute of Neuroscience and Medicine (INM-1), Research Center Juelich, Juelich, DE
 169 117. Amsterdam Public Health Institute, Vrije Universiteit Medical Center, Amsterdam, NL
 170 118. Centre for Integrative Biology, Università degli Studi di Trento, Trento, Trentino-Alto
 171 Adige, IT
 172 119. Department of Psychiatry and Psychotherapy, Medical Center, University of Freiburg,
 173 Faculty of Medicine, University of Freiburg, Freiburg, DE
 174 120. Psychiatry, Kaiser Permanente Northern California, San Francisco, CA, US
 175 121. Medical Research Council Human Genetics Unit, Institute of Genetics and Molecular
 176 Medicine, University of Edinburgh, Edinburgh, GB
 177 122. Department of Psychiatry, University of Toronto, Toronto, ON, CA
 178 123. Centre for Addiction and Mental Health, Toronto, ON, CA
 179 124. Division of Psychiatry, University College London, London, GB
 180 125. Neuroscience Therapeutic Area, Janssen Research and Development, LLC, Titusville,
 181 NJ, US
 182 126. Institute of Molecular and Cell Biology, University of Tartu, Tartu, EE
 183 127. Psychosis Research Unit, Aarhus University Hospital, Risskov, Aarhus, DK
 184 128. University of Liverpool, Liverpool, GB
 185 129. Mental Health Center Copenhagen, Copenhagen University Hospital, Copenhagen, DK
 186 130. Human Genetics and Computational Biomedicine, Pfizer Global Research and
 187 Development, Groton, CT, US
 188 131. Psychiatry, Harvard Medical School, Boston, MA, US
 189 132. Psychiatry, University of Iowa, Iowa City, IA, US
 190 133. Department of Psychiatry and Behavioral Sciences, Johns Hopkins University,
 191 Baltimore, MD, US
 192 134. Department of Psychiatry and Psychotherapy, University Medical Center Göttingen,
 193 Goettingen, Niedersachsen, DE
 194 135. Human Genetics Branch, NIMH Division of Intramural Research Programs, Bethesda,
 195 MD, US
 196 136. Faculty of Medicine, University of Iceland, Reykjavik, IS
 197 137. Child and Adolescent Psychiatry, Erasmus MC, Rotterdam, Zuid-Holland, NL
 198 138. Psychiatry, Erasmus MC, Rotterdam, Zuid-Holland, NL
 199 139. Psychiatry, Dalhousie University, Halifax, NS, CA
 200 140. Division of Epidemiology, New York State Psychiatric Institute, New York, NY, US
 201 141. Department of Clinical Medicine, University of Copenhagen, Copenhagen, DK
 202 142. Department of Medical & Molecular Genetics, King's College London, London, GB
 203 143. Psychiatry & Behavioral Sciences, Stanford University, Stanford, CA, US

204 144. NIHR BRC for Mental Health, King's College London, London, GB
205 145. Genetics, University of North Carolina at Chapel Hill, Chapel Hill, NC, US
206 146. Psychiatry, University of North Carolina at Chapel Hill, Chapel Hill, NC, US
207
208
209

determine variably methylated regions (**VMRs**): CpG-sites with **MAD-score** > **90th percentile** and at least 2 consecutive CpGs with at most 1kb distance

tagCpG: choose CpG-site with **highest MAD-score** within each VMR as representative

for each tagCpG

for all DeepSEA SNPs in 1MB cis distance to tagCpGs

for ten prenatal E

for ten prenatal E x DeepSEA SNPs in 1 MB cis of tag CpG

model G:
tagCpG ~ cis DeepSEA variants

keep model with lowest AIC across all G models

model E:
tagCpG ~ environmental phenotypes

keep model with lowest AIC across all E models

model G+E:
tagCpG ~ cis DeepSEA variants + environmental phenotypes

keep model with lowest AIC across all G +E models

model GxE:
tagCpG ~ cis DeepSEA variants x environmental phenotypes

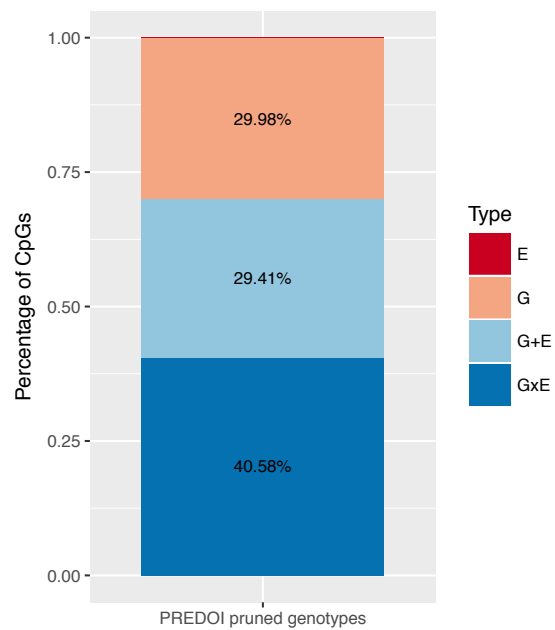
keep model with lowest AIC across all G x E models

determine **model with lowest AIC** across E, G, G+E and GxE models as **best model** for each tagCpG

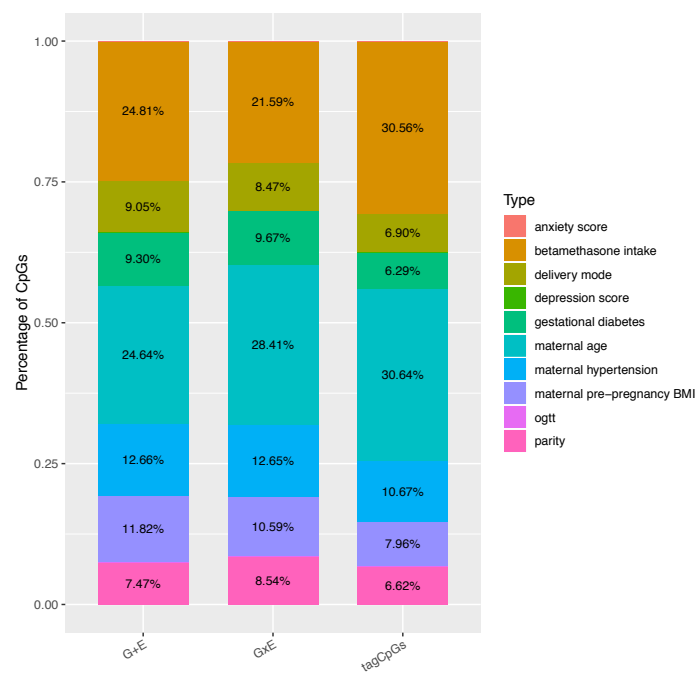
functional annotation of tagCpGs/DeepSEA variants stratified by best model E, G, G+E, GxE

replication of partition in best model E, G, G+E and GxE in independent cohorts

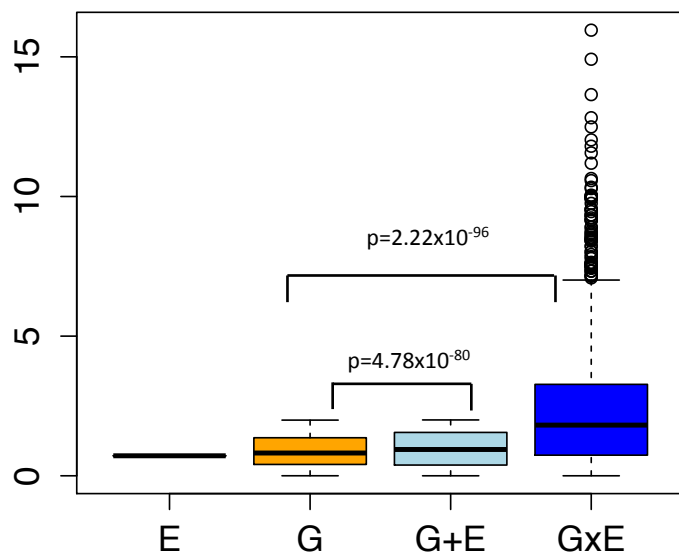
A

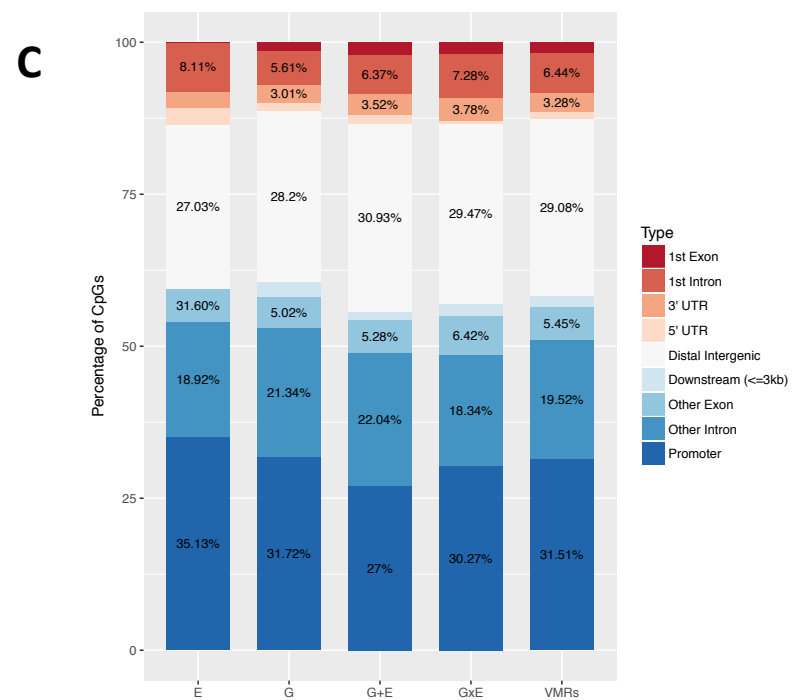
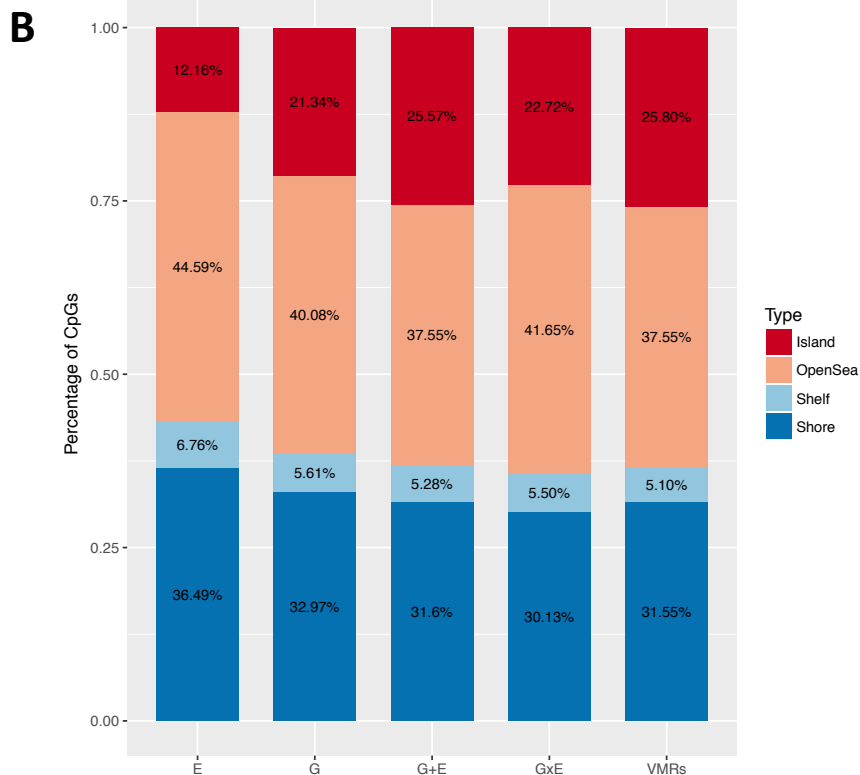
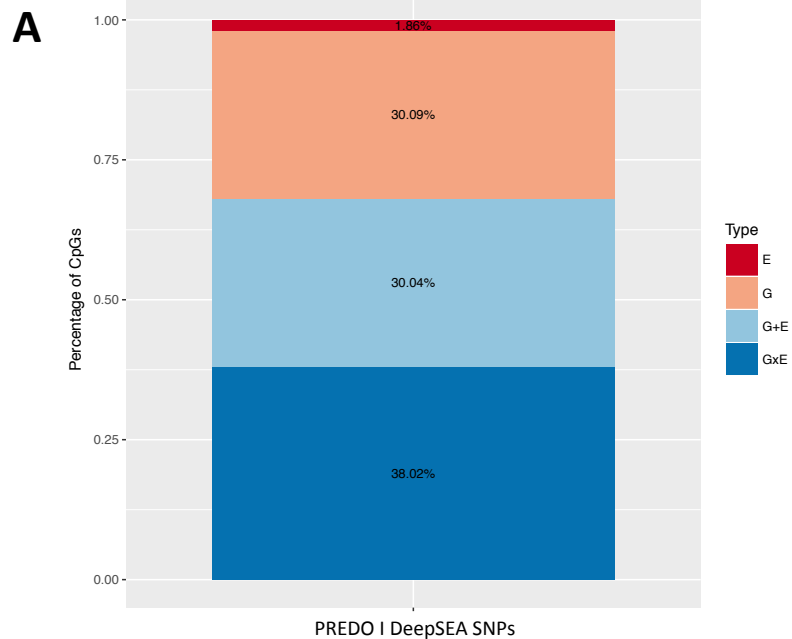


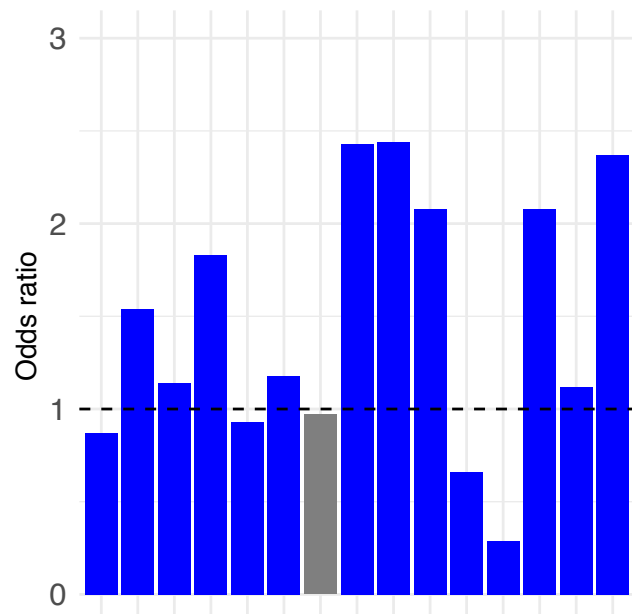
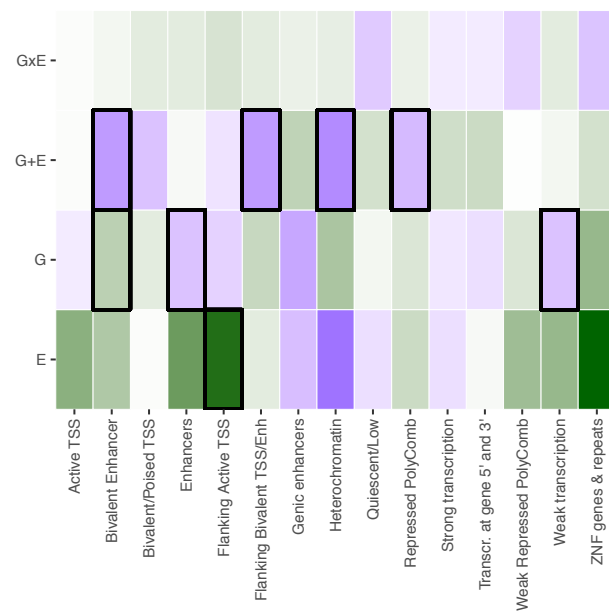
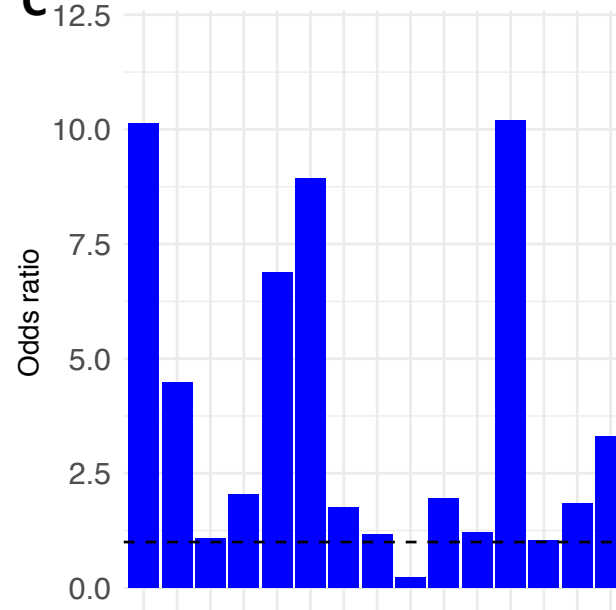
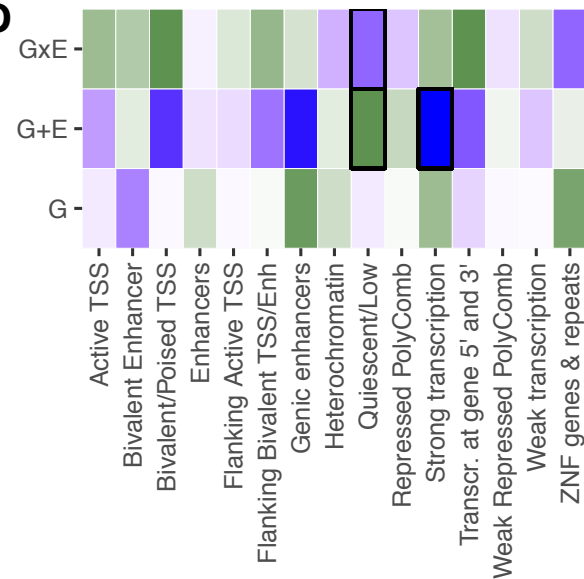
B



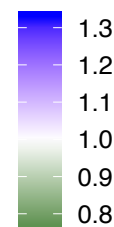
C

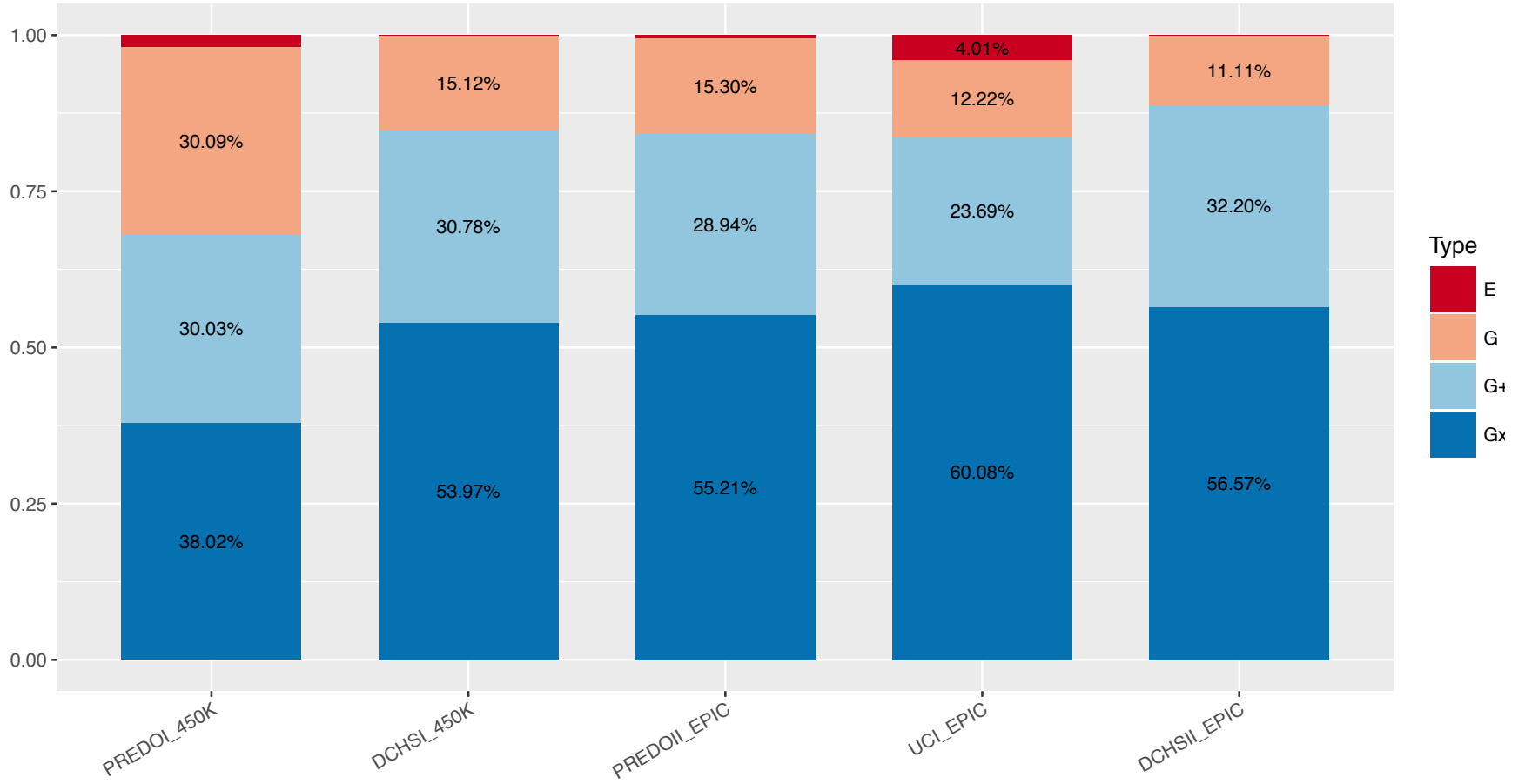


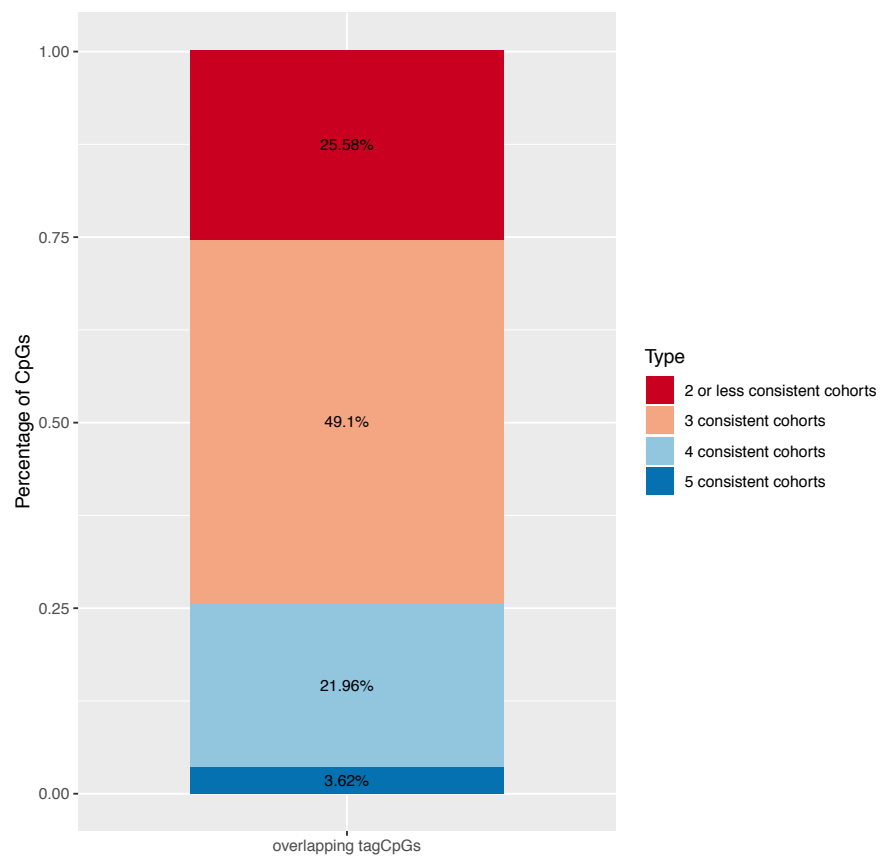


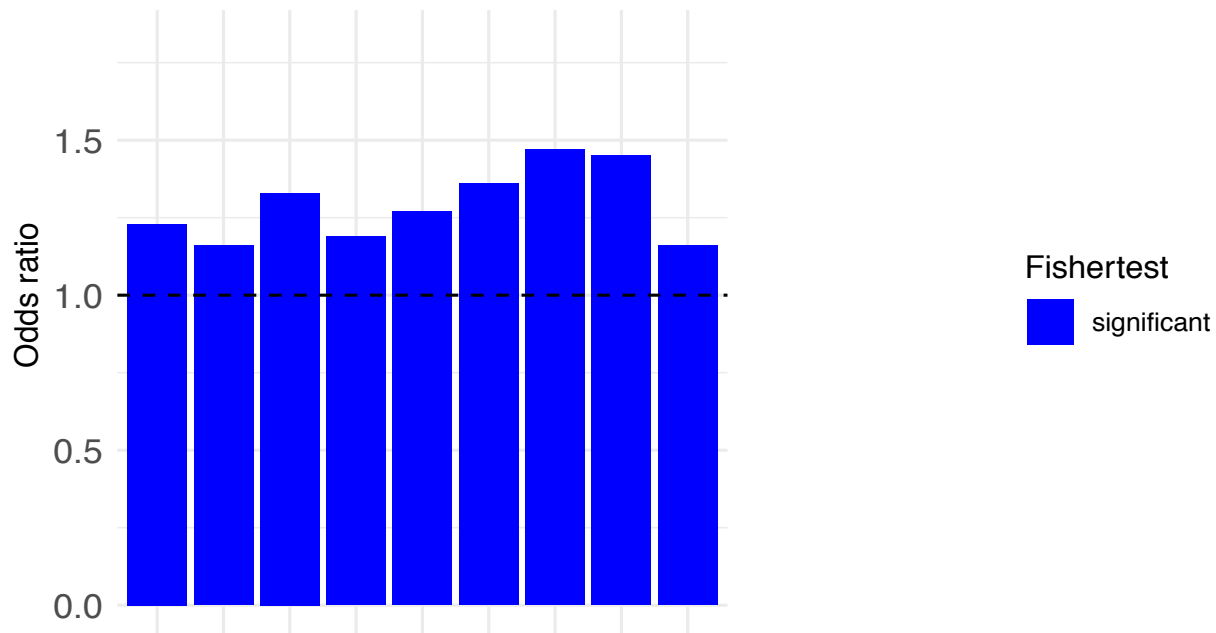
A**B****C****D**

not significant
significant

OR





A**B**